Chapter 3

Tracer correlation factor and atomic displacements due to the interstitialcy mechanism.

3.1 Introduction

A quantity of interest in studying atomic diffusion in solids due to point defects is the tracer correlation factor f and many calculations and simulations have been undertaken, for a wide range of systems (see for example Allnatt and Lidiard 1993 for a recent review). The tracer correlation factor characterises spatial correlations and the diffusion coefficient, D, can be written as $D = fD_{\mathrm{un}}$ where D_{un} is the diffusion coefficient for uncorrelated diffusion in the system (see for example LeClaire 1970; Kelly and Sholl 1987). If the theoretical values of the correlation factor for possible diffusion mechanisms are known, differences between the values of f can be used experimentally to help identify the dominant diffusion mechanisms present in a system.

A common model for diffusion in some systems is the interstitialcy mechanism. Diffusion by the interstitialcy mechanism occurs when an atom at an interstitial site moves on to a normal lattice site, pushing the atom at the normal lattice site on to an interstitial site. There may be several types of interstitialcy mechanisms possible in a particular system. The types are characterised by the angle between the original jump direction of the interstitial atom and the jump direction of the atom in moving from

its normal lattice site. If the interstitial atom and the normal atom move along the same straight line the diffusion is by the *collinear* interstitialcy mechanism. Otherwise the diffusion is by a *noncollinear* interstitialcy mechanism.

In the limit of low defect concentrations the correlation factor is sometimes a simple rational number: for example, $f = 1/2$ for the vacancy mechanism in the diamond structure and $f = 4/5$ for the collinear interstitialcy mechanism in the face-centred-cubic (f.c.c.) lattice. For the vacancy mechanism there is a simple explanation for such rational numbers. If an atom undergoes a jump in a particular direction the probability of the next jump of the atom occurring in the reverse direction is $2/Z$, where Z is the number of possible jump directions (Kelly and Sholl 1987). In cases where all other jump directions are equivalent, the probability of a jump in one of these directions is therefore $(1-2/Z)/(Z-1)$. The average cosine $c = \langle \cos\theta \rangle$ between successive jumps is therefore $c = -(2/Z) + (1 - 2/Z)c_1$ where $c_1 = \cos\theta_1$ and θ_1 is the angle between the original jump and one of the $Z - 1$ equivalent jumps. The correlation factor is then

$$f = \frac{1+c}{1-c} = (1 + c_1)/\left(\frac{Z+2}{Z-2} - c_1\right). \tag{3.1}$$

The rational numbers for f then follow immediately. For example, the diamond structure has $Z = 4$ and $c_1 = 1/3$ so that $f = 1/2$ and the two-dimensional honeycomb lattice has $Z = 3$ and $c_1 = 1/2$ so that $f = 1/3$. For cubic lattices the $Z - 1$ jumps are not equivalent so that this result does not apply, but if the approximation is made of assuming that the probability of each of the $Z - 1$ jumps occurring is the same for all of them, the well known approximation $f = 1 - 2/Z$ is obtained.

An aim of this chapter is to analyse the atom jump probabilities and correlation factors for the interstitialcy mechanism in a similar way. It is shown that the correlation factor in the case of the collinear interstitialcy mechanism has the simple form

$$f = 1 - \frac{1}{Z' - 1}, \tag{3.2}$$

where Z' is the number of possible jump directions for the interstitial defect. The results for the atom jump probabilities and the tracer correlation factor are also generalised to noncollinear interstitialcy mechanisms. The results obtained for f differ in their details for different systems, but are all of the same form which is a generalisation of equation (3.2).

The approach is to use the lattice generating functions (Green functions) to evaluate the appropriate atom jump probabilities. The method is similar to that recently used by Allnatt and Allnatt (1991) in analysing the correlation factor for the interstitialcy mechanism for the hexagonal lattice but calculates the atom jump probabilities in each direction directly. An advantage of evaluating the atom jump probabilities is that they also enable the atomic displacements due to a single atom-defect encounter to be evaluated (Sholl 1992) in cases where the encounter concept is valid. The encounter concept is valid at low defect concentrations in three-dimensional systems and the atomic diffusion can then be regarded as a random walk of independent encounters. In each encounter the atom will be displaced by a vector $\boldsymbol{l}$ with probability $W(\boldsymbol{l})$. Another aim of this chapter is to consider the evaluation of $W(\boldsymbol{l})$ for the interstitialcy mechanism which is used to evaluate the atomic displacement probabilities due to some interstitialcy mechanisms of self-diffusion in the NaCl structure as examples.

3.2 Atom jump probabilities

Expressions for the atom jump probabilities in terms of lattice generating functions are derived below for the special case of the collinear interstitialcy mechanism and then for the general interstitialcy mechanism of self-diffusion. The theory is exact for diffusion in the low defect-concentration limit.

3.2.1 Collinear interstitialcy mechanism

The collinear interstitialcy mechanism for diffusion corresponds to an interstitial defect first moving from an interstitial (I) site to a normal (N) lattice site and displacing the atom at the normal lattice site in the same direction to another interstitial site. The example of a square lattice is shown in Figure 3.1(a). The defect atom at the new position then jumps to any of its nearest neighbour normal lattice positions with equal probability and produces a further interstitial defect. The defect (not a particular atom) therefore moves on a particular lattice as shown in Figure 3.1(b) for the example of Figure 3.1(a). The defect can cause a further displacement of the original interstitial atom (now at a normal lattice site) if the defect moves through this atom position in either of two directions. The probability of the defect displacing the atom

in the reverse direction to its original I to N jump will be denoted Q_1 and the probability of the defect displacing the atom in the same direction as the original jump will be denoted Q_2. While the example shown in Figure 3.1 is a two-dimensional one, the same principles also apply to three-dimensional cases. In general there will be Z' nearest neighbour normal sites to a defect site, Z nearest neighbour defect sites to a normal site, and Z and Z' will not necessarily be equal.

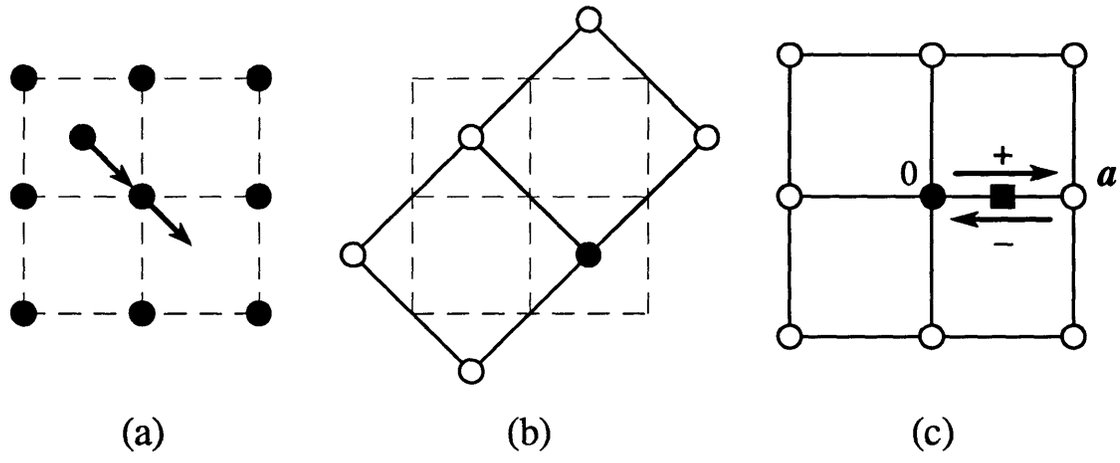

Figure 3.1: (a) The collinear interstitialcy mechanism in the square lattice. (b) The defect formed due to the jump in (a) can move on the lattice of sites shown as circles. (c) The parameters F_n^+ and F_n^- are the probabilities of a random walker passing through the square for the first time at the n^{th} step in the + and − directions respectively.

The atom jump probabilities Q_1 and Q_2 are related to the probability p of eventual return of the defect to the original atom by

$$Q_1 + Q_2 = p. \tag{3.3}$$

For two-dimensional systems $p = 1$ and $p < 1$ for three-dimensional systems. The parameters Q_1 and Q_2 are the jump probabilities for a particular defect-atom encounter and no other jump directions are possible due to this defect for a specific direction of the first jump as in Figure 3.1(a). At low defect concentrations in three-dimensional systems the effect of the second jump of an atom being due to a different defect must also be taken into account. If the jump is due to a different defect the jump will occur in each of the Z directions with probability $1/Z$. The jump probabilities in

the reverse and forward directions which also take account of other defects will be denoted q_1 and q_2 and

$$q_i = Q_i + \frac{1-p}{Z} \tag{3.4}$$

for $i = 1, 2$. The probabilities q_i for jumps in the other $Z-2$ directions are each $(1-p)/Z$ and the sum of q_i over all Z directions is 1.

The jump probabilities can be obtained by considering the random walk of the defect as in the example in Figure 3.1(b). The lattice on which the defect moves has been redrawn in Figure 3.1(c) and the required random walk problem can be stated in the following form. A random walker (the defect) starts at the origin and it is required to calculate the probability that it moves through the mid-point of a particular nearest neighbour step (the position of the atom) for the first time in either direction. Defining F_n to be the probability of a jump through this point for the first time at the n^{th} jump and F_n^+, F_n^- to be the probabilities of the jump occurring in the positive or negative directions respectively, the following equations relate these quantities and the jump probabilities.

$$F_n = F_n^+ + F_n^-, \tag{3.5}$$

$$p = \sum_{n=1}^{\infty} F_n = Q_1 + Q_2, \tag{3.6}$$

$$Q_1 = \sum_{n=1}^{\infty} F_n^+, \qquad Q_2 = \sum_{n=1}^{\infty} F_n^-. \tag{3.7}$$

The quantities F_n^+ and F_n^- can be expressed in terms of the probability function $P_n(\boldsymbol{l})$, which is the probability of the random walker being displaced by $\boldsymbol{l}$ in n steps, by the following equations.

$$F_n^+ = \frac{1}{Z'}\left[P_{n-1}(0) - \sum_{m=1}^{n-1} F_m^+ P_{n-m-1}(\boldsymbol{a}) - \sum_{m=1}^{n-1} F_m^- P_{n-m-1}(0)\right], \tag{3.8}$$

$$F_n^- = \frac{1}{Z'}\left[P_{n-1}(\boldsymbol{a}) - \sum_{m=1}^{n-1} F_m^+ P_{n-m-1}(0) - \sum_{m=1}^{n-1} F_m^- P_{n-m-1}(\boldsymbol{a})\right] \tag{3.9}$$

where $\boldsymbol{a}$ is a nearest neighbour lattice vector as in the example in Figure 3.1(c). These equations relate F_n^+ and F_n^- for the n^{th} jump to the possibilities at the $(n-1)^{\text{th}}$ jump and the probability $1/Z'$ of the n^{th} jump occurring in a particular direction. The functions $P_{n-1}(0)$ and $P_{n-1}(\boldsymbol{a})$ are the probabilities of the walker being in the required

position after the $(n-1)^{\text{th}}$ jump without considering the necessary restrictions that the target jump direction has not been traversed in the $(n-1)$ jumps. The remaining terms in the equation are a result of taking these restrictions into account.

Equations (3.8) and (3.9) can be expressed in terms of the corresponding generating functions by multiplying the equations by z^n and summing from 0 to ∞ taking account of the special cases $n = 0$ and 1. The equations then become, after choosing $z = 1$,

$$Z'Q_1 = P - Q_1P_1 - Q_2P, \tag{3.10}$$

$$Z'Q_2 = P_1 - Q_1P - Q_2P_1 \tag{3.11}$$

where the lattice generating functions P and P_1 for $z = 1$ are

$$P = \sum_{n=0}^{\infty} P_n(0), \tag{3.12}$$

$$P_1 = \sum_{n=0}^{\infty} P_n(\boldsymbol{a}). \tag{3.13}$$

Values of P are known for common structures and some values are (see for example Sholl 1981c; Ishioka and Koiwa 1978) 1.5163861 (simple-cubic), 1.3932039 (body-centred-cubic b.c.c.), 1.3446611 (f.c.c.) and 1.7928815 (diamond structure). The values of P_1 and p are related to P by $P_1 = P - 1$ and $P = 1/(1-p)$ (Sholl 1981c). The solution of equations (3.10) and (3.11) for Q_1 and Q_2 may then be written in the forms

$$Q_1 = \frac{Z'P}{(Z'-1)(2P+Z'-1)} = \frac{Z'}{2(Z'-1)} - \frac{1-p}{2}, \tag{3.14}$$

$$Q_2 = \frac{P(Z'-2) - Z' + 1}{(Z'-1)(2P+Z'-1)} = \frac{Z'-2}{2(Z'-1)} - \frac{1-p}{2}. \tag{3.15}$$

3.2.2 General interstitialcy mechanism

The general case of the interstitialcy mechanism corresponds to an interstitial defect atom moving from its interstitial (I) site on to a normal (N) lattice site, and displacing the atom at the normal site into a neighbouring interstitial site which need not be in the same direction, as in the special case of the collinear interstitialcy mechanism. The interstitial defect so formed is equally likely to then move to any of its Z' nearest neighbour normal lattice sites and produce a further interstitial defect. The defect

(not a particular atom) so moves on a lattice of interstitial sites according to the particular interstitialcy mechanism and will cause a further displacement of the atom if it returns to one of the Z interstitial sites adjacent to the atom and then moves on to the normal lattice site.

If the direction that an atom moves on its N to I jump is at an angle less than 180° to the direction of motion of the displacing interstitial atom, then the diffusion is by a noncollinear interstitialcy mechanism. There may be different types of noncollinear interstitialcy mechanisms possible in a particular system which correspond to different jump angles. For example, there are two types of noncollinear interstitialcy mechanisms of diffusion in the NaCl structure, a forward and a backward type, corresponding to angles of $\arccos(-1/3)$ and $\arccos(1/3)$ respectively (see Figure 3.2). For an atom at a normal lattice site that is displaced by an interstitial defect atom there are three possible jump directions for each of the two types of noncollinear interstitialcy mechanism on the NaCl structure.

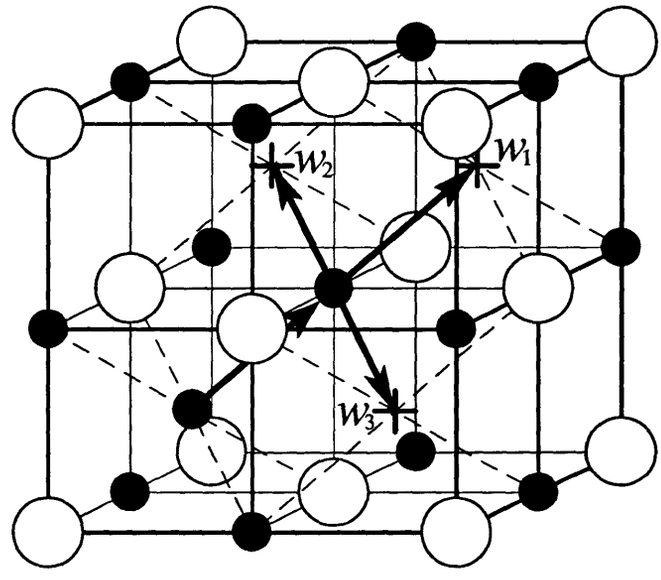

Figure 3.2: The three jump types in the NaCl structure associated with the jump-type probabilities w_1, w_2 and w_3. Shown are only one of each of the two noncollinear jump types possible for the interstitial atom, with the corresponding positions of the interstitial defect after the jump indicated by a +. There is one collinear jump type, with associated jump-type probability w_1. A solid circle represents a cation while an open circle represents an anion.

More generally, any of the interstitialcy jump types may be possible, each type with a probability w_i of occurring at each interstitialcy jump. The w_i satisfy the normalisation condition

$$\sum_i w_i = 1 \tag{3.16}$$

where the sum is over the different interstitialcy jump types. In this work w_1 is the probability that an interstitialcy jump is collinear and the w_i are ordered so that increasing i values correspond to smaller jump angles. In the NaCl structure, for example, the relevant probabilities are w_1, w_2 and w_3 and examples of the jump types shown in Figure 3.2. If a given interstitial jump type occurs then all possible jumps of that type of the normal atom are each equally likely.

An atom which is initially at a normal lattice site and is displaced to an interstitial site will then have a following jump to a normal site. Further jumps of the atom will depend upon the return of the interstitial defect. The I to N jumps of the atom will be equally likely to be to any of the Z' nearest normal lattice sites and the jumps are uncorrelated to any previous jumps of the atom. The N to I jumps of the atom, however, depend upon the direction from which the interstitial defect arrives at the normal site which, with the exception of the very first N to I jump, depends upon the previous I to N jump of the atom. In other words each N to I jump of an atom is correlated to its immediately preceding I to N jump.

It is convenient to define a composite lattice which consists of at least all of the normal lattice sites and all of the interstitial sites. The choice of this lattice is not unique. The diffusing atom therefore moves by nearest neighbour jumps on the composite lattice according to a model which corresponds to alternate N to I and I to N jumps. Not all of the sites on the composite lattice will be accessible to an atom starting at the origin.

A set of Z_T jump vectors $\boldsymbol{c}_i$ on the composite lattice can be defined as the union of the set of Z N to I jump vectors and Z' I to N jump vectors which represent all possible jumps of the atom on the composite lattice. The value of Z_T will be the larger of Z and Z' when one includes the other as a subset.

To describe the N to I jumps of an atom due to a particular atom-defect encounter, Q_{ij}^{N} is defined as the probability of an atom jumping from an N to I site in the direction $\boldsymbol{c}_i$ if its previous I to N jump was in the direction $\boldsymbol{c}_j$. This assumes that the defect

completes all its interactions with the atom before a second defect encounters the atom which is the case when there is just one interstitial defect present in the system; that is, in the low defect-concentration limit. The probability Q_{ij}^{N} describes the correlation between consecutive I to N and N to I jumps due to the differing probabilities of the defect returning to the atom from different directions. The values of the Q_{ij}^{N} are $Q_{ii}^{\mathrm{N}} = Q_2$, $Q_{ij}^{\mathrm{N}} = Q_1$ when i and j are such that $\boldsymbol{c}_j = -\boldsymbol{c}_i$, and the remaining Q_{ij}^{N} are zero for the collinear case. The probability p that the defect returns to displace the original atom is

$$p = \sum_{i=1}^{Z_T} Q_{ij}^{\mathrm{N}} \tag{3.17}$$

for any value of j. In two-dimensional systems $p = 1$ and the defect is always certain to return to the atom. The probability of return, $p < 1$ for three-dimensional systems and the mean number of atom jumps during the atom-defect encounter is finite. When more than one defect is present in the system the possibility of a second defect encountering the atom must be taken into account. The second defect is equally likely to approach the atom from any of the atom's Z nearest interstitial sites. The corresponding value of Q_{ij}^{N} for low concentrations of defects is then

$$q_{ij} = Q_{ij}^{\mathrm{N}} + \frac{1-p}{Z} \tag{3.18}$$

when the N to I jump is physically possible, which will not always be the case when $Z_T > Z$. Note that

$$\sum_{i=1}^{Z_T} q_{ij} = 1 \tag{3.19}$$

for any j. Knowledge of Q_{ij}^{N} is useful for the calculation of atom displacement probabilities $W(\boldsymbol{l})$ (discussed in §3.4) and for the calculation of the tracer correlation factor f. The correlation factor for the interstitialcy mechanism is $f = 1 + c$ (Le Claire and Lidiard 1956) where c is the average cosine for the angles between the directions of consecutive I to N and N to I jumps. Simple expressions for f as linear combinations of the Q_{ij}^{N} can be found for any system and the details depend upon the choice of definition of the $\boldsymbol{c}_i$ vectors (see §3.3).

The atom jump probabilities Q_{ij}^{N} can be determined by considering the uncorrelated random walk of the interstitial defect. If the atom of interest has just arrived at a normal lattice site, defined to be the origin, and the interstitial defect is at site

$\boldsymbol{c}_l$ then it is required to calculate the probability R_{kl} that the defect moves through the origin for the first time from the direction $-\boldsymbol{c}_k$. Defining u_{lj} as the probability an atom is displaced from its normal lattice site by $\boldsymbol{c}_l$ when displaced by an interstitial atom whose displacement is $\boldsymbol{c}_j$, the atom jump probabilities can be written, in matrix notation, as

$$\mathbf{Q} = \mathbf{uRu} \tag{3.20}$$

where Q^{N}_{ij}, u_{lj} and R_{kl} are the elements of the $Z_T \times Z_T$ square matrices $\mathbf{Q}$, $\mathbf{u}$ and $\mathbf{R}$ respectively. The u_{lj} can be written in terms of the interstitialcy jump-type probabilities w_i and the numbers α_i of distinct jumps possible, of type i, for an atom displaced by an interstitial atom from any particular direction. The u_{lj} are then w_i/α_i, with i chosen according to the definitions of $\boldsymbol{c}_l$ and $\boldsymbol{c}_j$. For example, u_{jj} corresponds to a collinear interstitialcy jump so that $u_{jj} = w_1/\alpha_1 = w_1$ since $\alpha_1 = 1$ for all lattice systems.

It is useful to define $F^k_n(\boldsymbol{c}_l)$, the probability that the interstitialcy defect passes through the origin for the first time on its n^{th} jump and that it approaches the origin in the direction $\boldsymbol{c}_k$ if it commenced its random walk from $\boldsymbol{c}_l$. The probability R_{kl} can be written

$$R_{kl} = \sum_{n=1}^{\infty} F^k_n(\boldsymbol{c}_l). \tag{3.21}$$

The first passage probability $F^k_n(\boldsymbol{c}_l)$ can in turn be expressed in terms of the probability function $P_n(\boldsymbol{l}_2, \boldsymbol{l}_1)$, the probability of the random walker being displaced from $\boldsymbol{l}_1$ to $-\boldsymbol{l}_2$ in n steps, by the equation

$$F^k_n(\boldsymbol{c}_l) = \frac{1}{Z'}\left[P_{n-1}(\boldsymbol{c}_k, \boldsymbol{c}_l) - \sum_{i,j=1}^{Z_T}\sum_{m=1}^{n-1} P_{n-m-1}(\boldsymbol{c}_k, \boldsymbol{c}_j) u_{ji} F^i_m(\boldsymbol{c}_l)\right]. \tag{3.22}$$

As in the equivalent equations for the special case of the collinear interstitialcy mechanism (equations (3.8) and (3.9)) the first term of the right hand side of this equation describes the probability the defect arrives at the required position after $n-1$ jumps, without the restriction that it cannot first pass through the origin, and the probability $1/Z'$ of the n^{th} jump taking the defect through the origin. The remaining terms of the equation are the result of taking the restriction into account.

Multiplying equation (3.22) by z^n and summing over n from 0 to ∞, taking account of the special cases $n = 0$ and 1, transforms the probability functions into

the corresponding probability generating functions. By setting $z = 1$ and using equation (3.21) for R_{kl} equation (3.22) becomes, in matrix notation,

$$\mathbf{R} = \frac{1}{Z'}\left[\mathbf{P} - \mathbf{PuR}\right] \tag{3.23}$$

where $\mathbf{P}$ is the $Z_T \times Z_T$ matrix with elements

$$P_{kl} = \sum_{n=0}^{\infty} P_n(\boldsymbol{c}_k, \boldsymbol{c}_l). \tag{3.24}$$

The probabilities P_{kl} correspond to random walks on the lattice of interstitial sites and the values of the probabilities are well known for random walks with nearest neighbour jumps on the cubic lattices and diamond structure (see for example Sholl 1981c; and Koiwa and Ishioka 1983). If the random walk involves other than just first nearest neighbour jumps on these or more complicated structures, the P_{kl} can be calculated as shown in Appendix D. The number of distinct P_{kl} will be less than Z_T^2 due to symmetry, the exact number being one greater than the number of interstitialcy jump types in general possible for the particular structure. These probabilities are denoted P_j, with $P_0 = P_{kk}$ being the probability generating function for zero displacement and P_j $(j > 0)$ the corresponding values for displacement to a j^{th} nearest neighbour site on the interstitial lattice. The exact details of the defect's random walk depend upon the interstitialcy jump-type probabilities w_i, and the probabilities P_j therefore also depend upon the w_i values.

Equation (3.20) and the solution of equation (3.23), for $\mathbf{R}$, give the final expression for the atom jump probabilities,

$$\mathbf{Q} = \frac{1}{Z'}\mathbf{u}\left[\mathbf{I} + \frac{1}{Z'}\mathbf{Pu}\right]^{-1}\mathbf{Pu} \tag{3.25}$$

where $\mathbf{I}$ is the $Z_T \times Z_T$ identity matrix. This is a key result of this work since—for a given structure and normalized jump-type probabilities w_i, and with the use of a standard numerical procedure to calculate the inverse matrix—it enables the rapid numerical calculation of the Q_{ij}^{N} once the values of the P_j are known.

Alternatively, expression (3.25) can be used to calculate the Q_{ij}^{N} algebraically in terms of the parameters Z', w_i, α_i and P_j, for particular structures. The major difficulty with this approach is to evaluate the inverse matrix in equation (3.25). This is straightforward for small matrices ($Z_T \leq 3$) but requires a symbolic mathematics

computer package for larger matrices. Matrices corresponding to values of $Z_T \leq 12$ are considered in this work and for $Z_T \geq 8$ the computation time can be significantly reduced by making use of the symmetry of the matrices and using block matrix techniques. In most cases the results for Q_{ij}^{N} are expressions which are too long to be of any practical use. On using these expressions and a symbolic mathematics computer package, however, remarkably simple expressions can be found for the tracer correlation factor f, as shown in the following section.

3.3 Tracer correlation factor

Presented below are analytic and numerical results for the tracer correlation factor f for diffusion in some cubic and two-dimensional systems.

Once the Q_{ij}^{N} have been calculated (from equation (3.25)), the tracer correlation factor, f, can be calculated using $f = 1 + c$ (LeClaire and Lidiard 1956) where c is the average cosine for the angles between consecutive I to N and N to I jumps. In terms of the atom jump probabilities, Q_{ij}^{N}, and jump vectors, $\boldsymbol{c}_i$, the expression for the average cosine between jumps is

$$c = \sum_{i=1}^{Z_T} q_{ij} \frac{\boldsymbol{c}_i \cdot \boldsymbol{c}_j}{|\boldsymbol{c}_i||\boldsymbol{c}_j|} = \sum_{i=1}^{Z_T} Q_{ij}^{\mathrm{N}} \frac{\boldsymbol{c}_i \cdot \boldsymbol{c}_j}{|\boldsymbol{c}_i||\boldsymbol{c}_j|} \tag{3.26}$$

which, in the present work, is independent of the value of j by symmetry. If the correlation factor is calculated from equations (3.25) and (3.26)—in terms of the Z', w_i, α_i and P_j, using a symbolic mathematics computer package—the result for the systems considered below is found, in all cases, to be of the form

$$f = 1 - \frac{AB^2}{\alpha(\alpha Z' - AB)} \tag{3.27}$$

where A is a linear combination of the P_j, B is a linear combination of the w_i, and α is equal to one or more of the α_i relevant to the particular system. A special case, in all the following systems where the collinear mechanism is possible, is the collinear interstitialcy mechanism ($w_1 = 1$) for which $A = 1$ and $B = \alpha$. In this case the expression for the correlation factor simplifies to

$$f = 1 - \frac{1}{Z' - 1}, \tag{3.28}$$

and the value depends only on the coordination number Z'. Alternatively, in terms of the Q_1, Q_2 notation of §3.2.1

$$f = 1 + c = 1 + Q_2 - Q_1 \tag{3.29}$$

and using expressions (3.14) and (3.15) for Q_1 and Q_2 the expression for the correlation factor again simplifies to equation (3.28). Since this result does not involve the lattice generating function P the results for f are simple fractions. Examples are $Z' = 6$ for the f.c.c. lattice so that $f = 4/5$ and $Z' = 4$ for the example in Figure 3.1(a) and for the NaCl structure so that $f = 2/3$.

The expression (3.28) for f is valid in the low defect concentration limit for collinear interstitialcy diffusion in one, two and three dimensions. For three dimensions this limit corresponds to defect concentrations low enough that each atom-defect encounter may be assumed to be completed before the atom is displaced by another defect. For one or two dimensions the low defect concentration limit is a single defect and in this case the probability p of return of the defect to a particular site is 1. In one dimension $Z' = 2$ and therefore $f = 0$. This is the correct result because long range diffusion is not then possible and $f = 0$ corresponds to a diffusion constant of zero.

The expressions for A, B and α for the general interstitialcy mechanism in some cubic and two-dimensional systems are as follows.

3.3.1 Systems with two interstitialcy jump types

The following systems each have two possible interstitialcy jump types. Two such two-dimensional systems are the square lattice where the interstitial lattice sites are either all in the centre of each square of normal lattice sites (for which $Z = Z' = 4$), or all on the midpoint between each pair of adjacent normal lattice sites (for which $Z = 4$ and $Z' = 2$). These systems will be denoted sq.(f) and sq.(e) respectively, where f(ace) and e(dge) refer to the positions of the interstitial sites in the normal lattice. Another example is the face-centred-cubic lattice with interstitial sites in the centre of the octahedra formed by the normal lattice sites (for which $Z = Z' = 6$) which has two interstitialcy jump types and will be referred to as f.c.c.(o). An example of such a system is the interstitialcy diffusion of cations in the CaF_2 structure. Also

considered is the simple-cubic lattice with interstitial sites on the midpoint between each pair of adjacent normal lattice sites (the edges of the cubes). An example is cationic interstitialcy diffusion in the CsCl structure where the interstitial sites are on the centre of each of the squares formed by the anion sites. This system has coordination numbers $Z = 6$ and $Z' = 2$, and will be referred to as s.c.(e).

For all of these systems the expressions for A, B and α, obtained by the method described in §3.2.2, are

$$\begin{aligned} A &= P_0 - P_2, \\ B &= w_1, \\ \alpha &= \alpha_1 = 1. \end{aligned} \tag{3.30}$$

The two types of interstitialcy jump mechanisms have associated probabilities w_1 and w_2, one of which, w_2, causes an N to I jump of the atom at right angles to its previous I to N jump and so does not contribute to the correlation factor. The case $w_1 = 0$ and $w_2 = 1$ which corresponds to strictly noncollinear jumps gives a tracer correlation factor $f = 1$. The other extreme, when $w_1 = 1$ and $w_2 = 0$, corresponds to collinear jumps and the probability generating functions satisfy $P_1 = 0$ and $P_2 = P_0 - 1$ since in this case the second nearest neighbour sites on the lattice of interstitial sites are now the nearest accessible sites to an interstitial defect.

Values of the P_j, Q_{ij}^{N} and f for some values of the jump-type probabilities, w_i, in the f.c.c.(o) and s.c.(e) structures are shown in Table 3.1. The values of the tracer correlation factor, f, for each structure range between the values for diffusion by the strictly collinear and the strictly noncollinear interstitialcy mechanisms. The probability generating functions P_0 and P_2 diverge for the case $w_1 = 1$, $w_2 = 0$ in the s.c.(e) system. The difference $P_0 - P_2$, however, is finite and its value is used to calculate the Q_{ij}^{N}.

3.3.2 Systems with three interstitialcy jump types

Two systems with three interstitialcy jump types will be considered. The first is a simple-cubic lattice where the interstitial sites are at the centre of each cube of normal lattice sites, for which $Z = Z' = 8$. This system will be referred to as s.c.(b) and an example is the interstitialcy diffusion of anions in the CaF_2 structure. The second

Table 3.1: Values of the probability generating functions, P_j, the atom jump probabilities, Q_{ij}^{N}, the probability, p, the defect returns to the atom, and the tracer correlation factor, f, for some values of the jump-type probabilities w_i, in the f.c.c.(o) and s.c.(e) systems. The angles shown with the Q_{ij}^{N} refer to the angles between consecutive I to N and N to I jumps of the atom. Also shown are the values of the tracer correlation factor obtained previously by the network resistance method (Compaan and Haven 1958).

f.c.c.(o)				
w_1, w_2	1,0	0,1	$\frac{1}{2},\frac{1}{2}$	$\frac{2}{3},\frac{1}{3}$
P_0	1.5163881	1.3446611	1.2065504	1.2081951
P_1	0	P_0-1	0.1961962	0.1560546
P_2	P_0-1	0.2299359	0.2169047	0.2342654
Q_{ij}^{N},(0°)	0.0265301	0.0682501	0.0257997	0.0165991
Q_{ij}^{N},(180°)	0.2265301	0.0682501	0.0707413	0.0974963
Q_{ij}^{N},(90°)	0	0.0483379	0.0431216	0.3552626
p	0.2530602	0.3298516	0.2690272	0.2561995
f	$\frac{4}{5}$	1	0.9550584	0.9191028
f (C&H)	0.8	1		

s.c.(e)				
w_1, w_2	1,0	0,1	$\frac{1}{2},\frac{1}{2}$	$\frac{2}{3},\frac{1}{3}$
P_0	$\rightarrow\infty$	1.4762128	1.4321661	1.5770988
P_1	0	P_0-1	0.3249602	0.2959571
P_2	P_0-1	0.3403122	0.5393720	0.7176697
Q_{ij}^{N},(0°)	0	0.1543307	0.0434145	0.0217582
Q_{ij}^{N},(180°)	1	0.1543307	0.1870796	0.2894218
Q_{ij}^{N},(90°)	0	0.0854431	0.0975246	0.0809408
p	1	0.6504338	0.6205926	0.6349431
f	0	1	0.8563349	0.7323364
f (C&H)	0	1		

system is a face-centred-cubic lattice with an interstitial site at the centre of each tetrahedron formed by adjacent normal lattice sites, for which $Z = 8$ and $Z' = 4$. This system will be referred to as f.c.c.(t) and an example is the interstitialcy diffusion of cations in the NaCl structure.

The expressions for A, B and α for both systems, obtained by the method described in §3.2.2, are

$$\begin{aligned} A &= P_0 + P_1 - P_2 - P_3, \\ B &= \alpha w_1 + w_2 - w_3, \\ \alpha &= \alpha_2 = \alpha_3 = 3. \end{aligned} \tag{3.31}$$

The P_j are for random walks on a simple-cubic lattice and have the same values for both systems except when w_1 is nonzero, since the third nearest neighbour jumps in the f.c.c.(t) system are subject to geometric restrictions not present in the s.c.(b) system. Table 3.2 shows values of the P_j, Q_{ij}^{N} and f for these systems and for some values of the normalised jump-type probabilities, w_i. The forward noncollinear jump mechanism ($w_2 = 1$, $w_1 = w_3 = 0$) gives $A = B = 1$ since $P_1 = P_3 = 0$ and $P_2 = P_0 - 1$ for the random walk with just second nearest neighbour jumps allowed, and the expression for the tracer correlation factor simplifies to

$$f = 1 - \frac{1}{\alpha(\alpha Z' - 1)}. \tag{3.32}$$

3.3.3 System with four interstitialcy jump types

A simple-cubic lattice of normal atoms and interstitial sites on the centre of each square formed by first and second nearest neighbour normal lattice sites has four types of interstitialcy jumps. An example of such a system is the interstitialcy diffusion of cations in the CsCl structure where the interstitial sites are on the midpoint between each pair of adjacent anion sites. This system has coordination numbers $Z = 12$ and $Z' = 4$, and will be referred to as s.c.(f).

The expressions for A, B and α for the s.c.(f) system, obtained by the method described in §3.2.2, are

$$A = P_0 + 2P_1 - 2P_3 - P_4,$$

Table 3.2: Values of the probability generating functions, P_j, the atom jump probabilities, Q_{ij}^{N}, the probability, p, the defect returns to the atom, and the tracer correlation factor, f, for some values of the jump-type probabilities w_i, in the f.c.c.(t) and s.c.(b) systems. The angles shown with the Q_{ij}^{N} refer to the angles between consecutive I to N and N to I jumps of the atom. Also shown are the values of the tracer correlation factor obtained previously by the network resistance method (Compaan and Haven 1958).

f.c.c.(t)						
w_1, w_2, w_3	1,0,0	0,1,0	0,0,1	$\frac{1}{3},\frac{1}{3},\frac{1}{3}$	$\frac{1}{2},\frac{1}{2},0$	$\frac{2}{3},\frac{1}{3},0$
P_0	1.7928802	1.3446611	1.5163863	1.1919798	1.1794606	1.2218536
P_1	0	0	P_0-1	0.2046404	0.1094808	0.0966143
P_2	0	P_0-1	0.3311489	0.1644149	0.1375198	0.1114850
P_3	P_0-1	0	0.2614704	0.2068841	0.2214014	0.2770379
Q_{ij}^{N},(0°)	0.0296478	0	0.0355398	0.0343943	0.0086974	0.0068888
Q_{ij}^{N},(180°)	0.3629812	0.1159541	0.1152852	0.0642197	0.1004157	0.1431404
Q_{ij}^{N},(70.5°)	0	0	0.0393915	0.0484203	0.0552229	0.0505024
Q_{ij}^{N},(109.5°)	0	0.0856511	0.0834193	0.0471037	0.0246501	0.0150698
p	0.3926290	0.3729075	0.5192575	0.3851857	0.3487319	0.3467457
f	$\frac{2}{3}$	$\frac{32}{33}$	0.9642823	0.9688580	0.8777089	0.8283158
f (C&H)	$\frac{2}{3}$	$\frac{32}{33}$	0.9643			

s.c.(b)						
w_1, w_2, w_3	1,0,0	0,1,0	0,0,1	$\frac{1}{3},\frac{1}{3},\frac{1}{3}$	$\frac{1}{2},\frac{1}{2},0$	$\frac{2}{3},\frac{1}{3},0$
P_0	1.3932033	1.3446611	1.5163863	1.1764894	1.1424630	1.1496816
P_1	0	0	P_0-1	0.2039071	0.1090663	0.0960538
P_2	0	P_0-1	0.3311489	0.1638124	0.1359402	0.1096152
P_3	P_0-1	0	0.2614704	0.1617486	0.1489857	0.1697149
Q_{ij}^{N},(0°)	0.0198412	0	0.0298275	0.0224221	0.0085847	0.0072199
Q_{ij}^{N},(180°)	0.1626984	0.0681662	0.0679226	0.0371410	0.0523883	0.0714125
Q_{ij}^{N},(70.5°)	0	0	0.0325413	0.0293452	0.0308237	0.0276058
Q_{ij}^{N},(109.5°)	0	0.0536734	0.0517666	0.0287401	0.0162226	0.0111434
p	0.1825396	0.2291864	0.3506737	0.2338190	0.2021119	0.1948797
f	$\frac{6}{7}$	$\frac{68}{69}$	0.9811302	0.9846760	0.9415953	0.9193450
f (C&H)		$\frac{68}{69}$				

$$B = \alpha w_1 + 2w_2 - 2w_4, \qquad (3.33)$$
$$\alpha = \alpha_2 = \alpha_4 = 4.$$

Table 3.3 shows values of the P_j, Q_{ij}^{N} and f for some values of the normalised jump-type probabilities w_i.

The two cases $w_1 = 1$ and $w_3 = 1$ (with the remaining $w_i = 0$ in each case) are equivalent to diffusion by the collinear and noncollinear interstitialcy mechanisms, respectively, on the square lattice system sq.(f). Since the lattice is two-dimensional, the interstitial defect is certain to return to the atom ($p = 1$) and the summation in the probability generating functions, P_j, diverges. The terms $P_0 - P_j$, however, remain finite (Montet 1973) and the values are shown in Table 3.3. The atom jump probabilities Q_{ij}^{N} can be calculated by writing their analytic expressions, from equation (3.25), in terms of the $P_0 - P_j$ and then allowing $P_0 \to \infty$. The results are shown in Table 3.3.

3.3.4 Systems with one interstitialcy jump type

Structures that permit just one possible interstitialcy jump type, a noncollinear one, are considered below. Two structures of this type are the two-dimensional hexagonal lattices with the interstitial sites either all at the centre of each hexagon of normal lattice sites (for which $Z = 3$ and $Z' = 6$) or all on the midpoint between each pair of adjacent normal lattice sites (for which $Z = 3$ and $Z' = 2$). Another is the lattice of Na^+ ions in the layered Na β-alumina structure whose Na^+ ions occupy every second site on a hexagonal lattice (forming a triangular lattice of normal sites) with the remaining sites of the hexagonal lattice the interstitial sites (for which $Z = Z' = 3$), (see for example Wolf 1979b).

For these systems $A = B = 1$ and the expression for the tracer correlation factor simplifies again to equation (3.32) with $\alpha = 2$ and the value of the correlation factor depends only on the coordination number Z'. This expression gives the same value of $f = 9/10$ obtained by Wolf (1979b) and Allnatt and Allnatt (1991) for diffusion by the interstitialcy mechanism in Na β-alumina with no site blocking. The atom jump probabilities Q_{ij}^{N} for a reverse (180°) jump and a forward noncollinear (60°) jump, in each of the above hexagonal systems, are $2Z'/[3(\alpha Z' - 1)]$ and $(2\alpha Z' - 1)/[3\alpha(\alpha Z' - 1)]$

Table 3.3: Values of the probability generating functions, P_j, the atom jump probabilities, Q_{ij}^{N}, the probability, p, the defect returns to the atom, and the tracer correlation factor, f, for some values of the jump-type probabilities w_i, in the s.c.(f) system. The angles shown wth the Q_{ij}^{N} refer to the angles between consecutive I to N and N to I jumps of the atom. Also shown are the values of the tracer correlation factor obtained previously by the network resistance method (Compaan and Haven 1958).

	s.c.(f)			
w_1, w_2, w_3, w_4	1,0,0,0	0,1,0,0	0,0,1,0	0,0,0,1
P_0	$\to \infty$	1.1326166	$\to \infty$	1.4762128
P_1	0	0.0704497	0	0.4762128
P_2	0	0.0762584	$P_0 - 1$	0.2971305
P_3	0	0.1326166	0	0.2539488
P_4	$P_0 - 1$	0.0542953	$P_0 - \frac{4}{\pi}$	0.2118984
Q_{ij}^{N},(0°)	$\frac{Z'-2}{2(Z'-1)} = \frac{1}{3}$	0.0068936	$\frac{\pi}{2\pi+4}$	0.0203843
Q_{ij}^{N},(180°)	$\frac{Z'}{2(Z'-1)} = \frac{2}{3}$	0.0734135	$\frac{\pi}{2\pi+4}$	0.0929297
Q_{ij}^{N},(90°)	0	0.0401535	$\frac{1}{\pi+2}$	0.0566570
Q_{ij}^{N},(60°)	0	0.0233506	0	0.0384767
Q_{ij}^{N},(120°)	0	0.0239391	0	0.0462062
p	1	0.3497726	1	0.5653600
f	$\frac{2}{3}$	0.9323030	1	0.9119956
f (C&H)	$\frac{2}{3}$	0.9323	1	0.9120
w_1, w_2, w_3, w_4	$\frac{1}{4},\frac{1}{4},\frac{1}{4},\frac{1}{4}$	$\frac{1}{3},\frac{1}{3},\frac{1}{3},0$	$\frac{1}{2},\frac{1}{2},0,0$	$\frac{2}{3},\frac{1}{3},0,0$
P_0	1.1453715	1.1598194	1.1412500	1.2049967
P_1	0.1370493	0.0824390	0.0695943	0.0635812
P_2	0.1778442	0.2058144	0.0548023	0.0458023
P_3	0.1080655	0.0895734	0.0862322	0.0728923
P_4	0.1585272	0.1840702	0.1962678	0.2710490
Q_{ij}^{N},(0°)	0.0277522	0.0252321	0.0050852	0.0056801
Q_{ij}^{N},(180°)	0.0441892	0.0629682	0.0905478	0.1376485
Q_{ij}^{N},(90°)	0.0359707	0.0441001	0.0145502	0.0091707
Q_{ij}^{N},(60°)	0.0314568	0.0177119	0.0097464	0.0069092
Q_{ij}^{N},(120°)	0.0319712	0.0329945	0.0443373	0.0391020
p	0.3975945	0.3792260	0.3410679	0.3457151
f	0.9825343	0.9316987	0.8453556	0.8036460

respectively. These values also, remarkably, depend only on the geometry of the system but not on the probability functions of the diffusion.

3.4 Atomic displacement probabilities

An atom which is initially at a normal lattice site and is displaced to an interstitial lattice site will then have a following jump to a normal site. This atom may then be displaced further due to the defect it creates in its second jump and the probability of the atom being displaced by $\boldsymbol{l}$ after n jumps will be denoted $W_n(\boldsymbol{l})$. The number of jumps, n, of the atom includes both N to I and I to N jumps and the atom will therefore be at an interstitial site after an odd number of jumps and at a normal site after an even number of jumps.

It is convenient to define $\boldsymbol{l}$ to be a lattice vector on the Bravais lattice which includes at least all of the normal and all of the interstitial lattice sites. Such a lattice will be termed a composite lattice and its choice is not unique. The diffusing atom therefore moves in steps on the composite lattice according to a model which corresponds to alternate N to I and I to N jumps and not all of the sites on this lattice will necessarily be accessible to an atom starting at the origin.

For one- and two-dimensional systems the defect has a probability $p = 1$ of returning to the atom. In three-dimensional systems $p < 1$ and in this case it is therefore possible to define $W(\boldsymbol{l})$ which is the probability of the atom being displaced by $\boldsymbol{l}$ as a result of a particular atom-defect encounter. Such an encounter will always involve an even number of atom jumps because an N to I jump of an atom will always be followed by an I to N jump. The atom will therefore be on a normal lattice site at the conclusion of the encounter. The probability that an encounter has exactly $2m$ jumps is equal to the probability that a defect returns to the atom $(m-1)$ times and then never returns again, which is $p^{m-1}(1-p)$, so that

$$W(\boldsymbol{l}) = (1-p)\sum_{m=1}^{\infty} p^{m-1} W_{2m}(\boldsymbol{l}). \tag{3.34}$$

The probabilities $W_n(\boldsymbol{l})$ can be evaluated by a generalisation of the analysis used by Sholl (1992) for the vacancy mechanism which used a recurrence relation between the n^{th} and $(n-1)^{\text{th}}$ jumps. For the interstitial mechanism it is also necessary to distinguish between N to I and I to N jumps.

A set of Z_T jump vectors $\boldsymbol{c}_i$ on the composite lattice can be defined such that they include all possible I to N jumps and all possible N to I jumps. The value of Z_T will be the larger of Z and Z' when one set of jumps includes the other as a sub-set. The expression for $W(\boldsymbol{l})$ can then be written

$$W(\boldsymbol{l}) = (1-p)\sum_{m=1}^{\infty} p^{m-1} \sum_{i=1}^{Z_T} W_{2m}(\boldsymbol{l}, \boldsymbol{c}_i) \tag{3.35}$$

where $W_{2m}(\boldsymbol{l}, \boldsymbol{c}_i)$ is the probability $W_{2m}(\boldsymbol{l})$ with the restriction that the $2m^{\text{th}}$ jump be in the direction $\boldsymbol{c}_i$. The probability that an N to I jump of an atom is in the direction $\boldsymbol{c}_i$ if the immediately preceding I to N jump was in the direction $\boldsymbol{c}_j$ is denoted Q^{N}_{ij}. This probability describes the correlation between consecutive I to N and N to I jumps due to the differing probabilities of the defect returning to the atom from different directions. The values of the Q^{N}_{ij} are $Q^{\mathrm{N}}_{ii} = Q_2$, $Q^{\mathrm{N}}_{ij} = Q_1$ when i and j are such that $\boldsymbol{c}_j = -\boldsymbol{c}_i$, and the remaining Q^{N}_{ij} are zero for the collinear case.

The I to N jumps of the atom are completely uncorrelated to any previous jump and the atom is equally likely to jump to any of its Z' nearest normal lattice sites, each with probability $1/Z'$. When Z' is less than Z there will be (Z/Z') different sets of Z' possible jump directions available to an atom at an interstitial site. It is convenient to define Q^{I}_{ij} to indicate the probability of a jump in the direction $\boldsymbol{c}_i$ for an atom at an interstitial site. Q^{I}_{ij} will be equal to $1/Z'$ if an I to N jump in the direction $\boldsymbol{c}_i$ is possible, or 0 if it is not possible, given that the previous N to I jump was in the direction $\boldsymbol{c}_j$. This is equivalent to $Q^{\mathrm{I}}_{ij} = 1/Z'$ for all values of i for which the lattice vector $(\boldsymbol{c}_i + \boldsymbol{c}_j)$ is a nearest normal lattice site to the interstitial site $\boldsymbol{c}_j$, and zero otherwise. For the case $Z' \geq Z$ the possible jump directions will be the same from any interstitial site, so that $Q^{\mathrm{I}}_{ij} = 1/Z'$ for all i and j values. In all cases

$$\sum_{i=1}^{Z_T} Q^{\mathrm{I}}_{ij} = 1. \tag{3.36}$$

Using the above definitions the following recurrence relations hold.

$$W_{2m}(\boldsymbol{l}, \boldsymbol{c}_i) = \sum_{j=1}^{Z_T} Q^{\mathrm{I}}_{ij} W_{2m-1}(\boldsymbol{l} - \boldsymbol{c}_i, \boldsymbol{c}_j), \tag{3.37}$$

$$W_{2m+1}(\boldsymbol{l}, \boldsymbol{c}_i) = \frac{1}{p} \sum_{j=1}^{Z_T} Q^{\mathrm{N}}_{ij} W_{2m}(\boldsymbol{l} - \boldsymbol{c}_i, \boldsymbol{c}_j) \tag{3.38}$$

with $m \geq 1$ in both equations; the initial condition is

$$W_1(\boldsymbol{l}, \boldsymbol{c}_i) = \frac{1}{Z}\delta_{\boldsymbol{l},\boldsymbol{c}_i}. \tag{3.39}$$

Equations (3.37) and (3.38) can be combined to give the recurrence relation

$$W_{2m}(\boldsymbol{l}, \boldsymbol{c}_i) = \frac{1}{p}\sum_{j,k=1}^{Z_T} Q^{\mathrm{I}}_{ik} Q^{\mathrm{N}}_{kj} W_{2m-2}(\boldsymbol{l} - \boldsymbol{c}_i - \boldsymbol{c}_k, \boldsymbol{c}_j) \tag{3.40}$$

which may be solved using the matrix and Fourier transform procedure of Sholl (1992). The Fourier transform of $W(\boldsymbol{l})$ is

$$W(\boldsymbol{\phi}) = \frac{(1-p)}{Z}\sum_{i,j,k=1}^{Z_T} Q^{\mathrm{I}}_{jk}\left[\mathbf{I} - p\mathbf{A}(\boldsymbol{\phi})\right]^{-1}_{ij} \exp[i\boldsymbol{\phi}\cdot(\boldsymbol{c}_j + \boldsymbol{c}_k)], \tag{3.41}$$

and the final solutions are

$$W(\boldsymbol{l}) = \frac{(1-p)}{Z}\frac{v}{(2\pi)^3}\int \sum_{i,j,k=1}^{Z_T} Q^{\mathrm{I}}_{jk}\left[\mathbf{I} - p\mathbf{A}(\boldsymbol{\phi})\right]^{-1}_{ij} \exp\{-i\boldsymbol{\phi}\cdot[\boldsymbol{l} - (\boldsymbol{c}_j + \boldsymbol{c}_k)]\}\, d\boldsymbol{\phi}, \tag{3.42}$$

$$W_{2m}(\boldsymbol{l}) = \frac{1}{Z}\frac{v}{(2\pi)^d}\int \sum_{i,j,k=1}^{Z_T} Q^{\mathrm{I}}_{jk}\left[\mathbf{A}^{m-1}(\boldsymbol{\phi})\right]_{ij} \exp\{-i\boldsymbol{\phi}\cdot[\boldsymbol{l} - (\boldsymbol{c}_j + \boldsymbol{c}_k)]\}\, d\boldsymbol{\phi}, \tag{3.43}$$

and

$$W_{2m+1}(\boldsymbol{l}) = \frac{1}{pZ}\frac{v}{(2\pi)^d}\int \sum_{h,i,j,k=1}^{Z_T} Q^{\mathrm{I}}_{hk} Q^{\mathrm{N}}_{ij}\left[\mathbf{A}^{m-1}(\boldsymbol{\phi})\right]_{jh} \exp\{-i\boldsymbol{\phi}\cdot[\boldsymbol{l} - (\boldsymbol{c}_h + \boldsymbol{c}_i + \boldsymbol{c}_k)]\}\, d\boldsymbol{\phi} \tag{3.44}$$

where $m \geq 1$, $\mathbf{I}$ is the $Z_T \times Z_T$ identity matrix, $\mathbf{A}(\boldsymbol{\phi})$ is the square matrix with elements

$$[\mathbf{A}(\boldsymbol{\phi})]_{ij} = \frac{1}{p}\sum_{k=1}^{Z_T} Q^{\mathrm{I}}_{ik} Q^{\mathrm{N}}_{kj} \exp[i\boldsymbol{\phi}\cdot(\boldsymbol{c}_i + \boldsymbol{c}_k)], \tag{3.45}$$

and the integral is over the first Brillouin zone of the reciprocal lattice of the composite Bravais lattice. The dimension of the lattice is d and v is the volume of the unit cell. The integrals in the above expressions may be evaluated numerically for a given lattice structure and vector $\boldsymbol{l}$.

An example of the above theory is the collinear interstitialcy diffusion of the cations in the NaCl structure. In this case the interstitial cation sites are at the centres of tetrahedra of both the cations and anions (a f.c.c.(t) system). The number of N (cation) sites which are nearest neighbours of an I site is therefore $Z' = 4$ and the

number of I sites which are nearest neighbours of an N site is $Z = 8$. The composite lattice may be chosen as the b.c.c. lattice comprising all of the anion, cation and interstitial sites. The set of vectors $\boldsymbol{c}_i$ are the eight nearest neighbour vectors of a b.c.c. lattice site. If the $\boldsymbol{c}_i$ are labelled so that $\boldsymbol{c}_{i+1} = -\boldsymbol{c}_i$ for $i = 1, 3, 5, 7$ and

$$\boldsymbol{c}_1 = \frac{a}{4}(1,1,1), \quad \boldsymbol{c}_3 = \frac{a}{4}(1,-1,-1), \quad \boldsymbol{c}_5 = \frac{a}{4}(-1,-1,1), \quad \boldsymbol{c}_7 = \frac{a}{4}(-1,1,-1) \tag{3.46}$$

relative to orthogonal axes, where a is the NaCl lattice parameter, then

$$Q^{\mathrm{I}}_{ij} = \frac{1}{4}\delta_{1,(-)^{i+j+1}} \tag{3.47}$$

$$Q^{\mathrm{N}}_{ii} = Q_2, \quad Q^{\mathrm{N}}_{j,j+1} = Q^{\mathrm{N}}_{j+1,j} = Q_1 \quad (j = 1,3,5,7) \tag{3.48}$$

with the remaining Q^{N}_{ij} zero. The interstitial defect moves on one of four diamond structures for which the probability parameters P and p are $P = 1.7928815$ and $p = 0.3926292$. From equations (3.14) and (3.15) the probabilities Q_1 and Q_2 of backward and forward jumps are $Q_1 = 0.3629813$ and $Q_2 = 0.0296479$. The results for the displacement probabilities $W(\boldsymbol{l})$ of an atom as a result of a single atom-defect encounter may then be obtained from equation (3.42) and some values are given in Table 3.4. The results show that the atom is most likely to be at the origin or at a nearest neighbour site as a result of the encounter. The probability of it being at the origin is 0.241 and at a nearest neighbour site is 0.732 so that the probability of it being at other sites is only 0.027.

The correlation factor f can be expressed in terms of the probabilities $W(\boldsymbol{l})$ (Wolf 1983) and the result for the interstitialcy mechanism can be derived as follows. The correlation factor f is

$$f = \lim_{n\to\infty} \frac{\langle \boldsymbol{R}^2 \rangle_n}{nb^2} \tag{3.49}$$

where $\langle \boldsymbol{R}^2 \rangle_n$ is the mean square displacement of an atom after n jumps, b is the length of each jump and nb^2 is the mean square displacement if the jumps are uncorrelated. For the interstitialcy mechanism n includes all I to N and N to I jumps and b is the I to N separation. Since different atom-defect encounters are uncorrelated, it follows that

$$\langle \boldsymbol{R}^2 \rangle_n = n_e \langle \boldsymbol{R}^2 \rangle_{enc} = n_e \sum_{\boldsymbol{l}} W(\boldsymbol{l}) l^2 \tag{3.50}$$

Table 3.4: Values of the displacement probability $W(\boldsymbol{l})$ greater than 10^{-7} for representative nearest neighbours and cumulative sums over shells of neighbours of $W(\boldsymbol{l})$ and the correlation factor f for self-diffusion in the NaCl structure. The coordinates of $\boldsymbol{l}$ are relative to orthogonal axes and are in units of $a/2$.

$\boldsymbol{l}$	$W(\boldsymbol{l})$	$\sum_{\boldsymbol{l}} W(\boldsymbol{l})$	$f = P^{-1}\sum_{\boldsymbol{l}} W(\boldsymbol{l})\,(l/b)^2$
0,0,0	0.2412699	0.2412699	0
0,1,1	0.0610196	0.9735048	0.5929841
1,1,2	0.0007104	0.9905538	0.6344045
0,2,2	0.0007268	0.9992757	0.6626572
0,1,3	0.0000085	0.9994787	0.6634795
1,2,3	0.0000084	0.9998803	0.6657556
0,0,4	0.0000004	0.9998826	0.6657710
0,3,3	0.0000083	0.9999819	0.6664943
1,1,4	0.0000002	0.9999866	0.6665283
2,3,3	0.0000001	0.9999890	0.6665336
2,2,4	0.0000002	0.9999936	0.6665451
1,3,4	0.0000001	0.9999983	0.6665574
0,4,4	0.0000001	0.9999995	0.6666599
		$\sum_{\boldsymbol{l}} W(\boldsymbol{l}) = 1$	$f = 2/3$

where $\langle \boldsymbol{R}^2 \rangle_{enc}$ is the mean square displacement of an atom as a result of a single encounter and n_e is the average number of encounters in n atom jumps. The values of n_e and n are related by $n = Pn_e$ since the mean number of atom jumps per encounter is equal to the lattice generating function P (Sholl 1992). The expression for f may then be written in the form

$$f = \frac{1}{P}\sum_{\boldsymbol{l}} W(\boldsymbol{l}) \left(\frac{l}{b}\right)^2 . \tag{3.51}$$

For the example of the NaCl structure the jump distance $b = \sqrt{3}a/4$ and the cumulative sum in equation (3.51) is given in Table 3.4. The convergence of this summation is relatively slow because of the l^2 term but the rate of convergence in Table 3.4 is faster than the case of the vacancy mechanism in the simple cubic lattice (Sholl 1992).

Some examples of the atomic displacement probability, $W(\boldsymbol{l})$, for the noncollinear interstitialcy mechanism are given below, where the values of the atom jump probabilities, Q_{ij}^{N}, used in calculating the $W(\boldsymbol{l})$ are calculated from equation (3.25) and are given in Tables 3.2 and 3.3. Table 3.5 shows the results of these calculations for self-diffusion by the interstitialcy mechanism in the NaCl structure for various values of the jump-type probabilities w_i. As can be seen in the table, the rate of reduction in $W(\boldsymbol{l})$ as the distance from the origin is increased is greater for diffusion corresponding to smaller values of the tracer correlation factor. The results of similar calculations for the CsCl structure, s.c.(f), given in Table 3.6 show that a similar correlation exists between the rate of reduction in $W(\boldsymbol{l})$ and the value of the tracer correlation factor. This result is to be expected physically since a smaller value of f corresponds to a higher probability of an atom having a reverse jump following a given jump. This will then inhibit the atom from diffusing far from its starting point.

3.5 Conclusion

A matrix expression for the atom jump probabilities Q_{ij}^{N} for the interstitialcy diffusion mechanism has been obtained (equation (3.25)) in terms of the interstitialcy jump-type probabilities w_i and the probability generating functions P_j for the random walk of the interstitial defect. This expression enables the calculation of the Q_{ij}^{N} for any interstitialcy mechanism once the corresponding P_j are known. The techniques for calculating the probability generating functions P_j, for a given set of w_i values, are outlined in Appendix D.

The tracer correlation factor f can be calculated from the Q_{ij}^{N} and the direction cosines. With the aid of a symbolic mathematics computer package the analytic expressions for the correlation factor—in terms of the parameters Z', α_i, w_i and P_j—were found for some cubic and two-dimensional systems. The general form of the correlation factor was

$$f = 1 - \frac{AB^2}{\alpha(\alpha Z' - AB)} \tag{3.52}$$

where A, B and α are linear combinations of the P_j, w_i and α_i respectively, and the expressions for A, B and α for specific systems are given by equations (3.30) to (3.33).

It is not obvious that a simple general expression for the tracer correlation factor

Table 3.5: Values of the displacement probability $W(\boldsymbol{l})$ greater than 10^{-7} for representative nearest neighbours for self-diffusion by the interstitialcy mechanism in the NaCl structure, f.c.c.(t). The $W(\boldsymbol{l})$ are for a few choices of the jump-type probabilities, w_i, and the corresponding values of the trace correlation factor, f, are shown. The coordinates of $\boldsymbol{l}$ are relative to orthogonal axes and are in units of $a/2$.

w_1,w_2,w_3	0,1,0	$\frac{1}{3},\frac{1}{3},\frac{1}{3}$	$\frac{1}{2},\frac{1}{2},0$	1,0,0
$\boldsymbol{l}$	$f=\frac{32}{33}$	$f=0.9688580$	$f=0.8777089$	$f=\frac{2}{3}$
0,0,0	0.1933076	0.2000786	0.2061602	0.2412699
0,1,1	0.0549503	0.0561546	0.0574003	0.0610196
0,0,2	0.0056541	0.0053578	0.0054376	
1,1,2	0.0030570	0.0026521	0.0022041	0.0007104
0,2,2	0.0016589	0.0013157	0.0008384	0.0007268
0,1,3	0.0003515	0.0002748	0.0002147	0.0000085
2,2,2	0.0002433	0.0001777	0.0001062	
1,2,3	0.0001384	0.0000959	0.0000528	0.0000084
0,0,4	0.0000368	0.0000253	0.0000179	0.0000004
0,3,3	0.0000551	0.0000342	0.0000144	0.0000083
1,1,4	0.0000259	0.0000169	0.0000102	0.0000002
0,2,4	0.0000183	0.0000114	0.0000059	
2,3,3	0.0000140	0.0000083	0.0000034	0.0000001
2,2,4	0.0000084	0.0000048	0.0000019	0.0000002
1,3,4	0.0000060	0.0000033	0.0000012	0.0000001
0,1,5	0.0000028	0.0000016	0.0000009	
1,2,5	0.0000016	0.0000008	0.0000003	
0,4,4	0.0000020	0.0000010	0.0000003	0.0000001
0,3,5	0.0000009	0.0000004	0.0000001	
3,3,4	0.0000010	0.0000005	0.0000001	
2,4,4	0.0000007	0.0000003	0.0000001	
0,0,6	0.0000003	0.0000001	0.0000001	
2,3,5	0.0000005	0.0000002	0.0000001	
1,1,6	0.0000002	0.0000001		
0,2,6	0.0000002	0.0000001		
1,4,5	0.0000003	0.0000001		
2,2,6	0.0000001			
1,3,6	0.0000001			
4,4,4	0.0000001			
0,5,5	0.0000001			
3,4,5	0.0000001			

Table 3.6: Values of the displacement probability $W(\boldsymbol{l})$ as in Table 3.5 but for self-diffusion by the interstitialcy mechanism in the CsCl structure, s.c.(f). The coordinates of $\boldsymbol{l}$ are relative to orthogonal axes and are in units of a, the lattice parameter.

w_1,w_2,w_3,w_4	$\frac{1}{4},\frac{1}{4},\frac{1}{4},\frac{1}{4}$	0,1,0,0	$\frac{1}{3},\frac{1}{3},\frac{1}{3},0$	$\frac{1}{2},\frac{1}{2},0,0$
$\boldsymbol{l}$	$f = 0.9825343$	$f = 0.9323030$	$f = 0.9316987$	$f = 0.8453556$
0,0,0	0.1866267	0.2013738	0.1952846	0.2088675
0,0,1	0.0691846	0.0729378	0.0716308	0.0751945
0,1,1	0.0220691	0.0219932	0.0221246	0.0227636
1,1,1	0.0043950	0.0034026	0.0037058	0.0038270
0,0,2	0.0036108	0.0030431	0.0033873	0.0015243
0,1,2	0.0017363	0.0012942	0.0014734	0.0006964
1,1,2	0.0007409	0.0004997	0.0005138	0.0002964
0,2,2	0.0003478	0.0001661	0.0002785	0.0000859
0,0,3	0.0002154	0.0001385	0.0001741	0.0000352
1,2,2	0.0001424	0.0000733	0.0000883	0.0000364
0,1,3	0.0001287	0.0000731	0.0000933	0.0000201
1,1,3	0.0000738	0.0000381	0.0000451	0.0000114
2,2,2	0.0000368	0.0000165	0.0000188	0.0000063
0,2,3	0.0000382	0.0000149	0.0000258	0.0000044
1,2,3	0.0000211	0.0000082	0.0000114	0.0000025
0,0,4	0.0000141	0.0000067	0.0000095	0.0000009
0,1,4	0.0000096	0.0000041	0.0000059	0.0000006
2,2,3	0.0000063	0.0000022	0.0000029	0.0000006
1,1,4	0.0000064	0.0000025	0.0000034	0.0000004
0,3,3	0.0000068	0.0000019	0.0000042	0.0000004
1,3,3	0.0000039	0.0000012	0.0000019	0.0000003
0,2,4	0.0000036	0.0000011	0.0000020	0.0000002
1,2,4	0.0000024	0.0000007	0.0000011	0.0000001
2,3,3	0.0000014	0.0000004	0.0000005	0.0000001
2,2,4	0.0000009	0.0000002	0.0000004	
0,0,5	0.0000010	0.0000003	0.0000005	
0,3,4	0.0000009	0.0000002	0.0000005	
0,1,5	0.0000007	0.0000002	0.0000004	
1,3,4	0.0000006	0.0000001	0.0000002	
1,1,5	0.0000005	0.0000002	0.0000002	
3,3,3	0.0000003	0.0000001	0.0000001	
0,2,5	0.0000003	0.0000001	0.0000002	
2,3,4	0.0000002		0.0000001	
1,2,5	0.0000002	0.0000001	0.0000001	
0,4,4	0.0000002		0.0000001	
2,2,5	0.0000001			
1,4,4	0.0000001			
0,3,5	0.0000001			
3,3,4	0.0000001			
1,3,5	0.0000001			
0,0,6	0.0000001			
0,1,6	0.0000001			

should exist as the diffusion mechanism is quite a complicated process. Many of the methods used previously to calculate the tracer correlation factor lead to numerical calculations which must be performed each time for a different mechanism: for example, the extensively used network-resistance method of Compaan and Haven (1958). The method used here shows that simple general expressions exist for all combinations of interstitialcy mechanisms. A crucial part of this method was the use of a symbolic mathematics computer package which performed the involved algebra in terms of the parameters Z', α_i, w_i and P_j. Of these, the w_i and P_j have non-integer values which mask the general form of f when calculated numerically.

Despite the complexities of the possible diffusion paths of an interstitial defect in producing diffusion of an atom by the collinear interstitialcy mechanism, the tracer correlation factor depends only on the number Z' of normal lattice sites which are nearest neighbours of the defect site and is given by $f = 1 - 1/(Z' - 1)$. This result is valid in one, two and three dimensions in the limit of low defect concentrations. The correlation factor therefore depends simply on the geometry of the interstitial and normal lattice sites and does not depend explicitly on any details of the diffusion motion.

The results derived for the atom jump probabilities enable the probability of an atom being displaced by $\boldsymbol{l}$ in n jumps to be obtained from the integral expressions (3.43) and (3.44). For three-dimensional systems the mean number of exchanges between an atom and a particular defect is finite and the final atomic displacement probability $W(\boldsymbol{l})$ as a result of such an atom-defect encounter can also be obtained from the integral expression (3.42).

Chapter 4

Relaxation rates due to the vacancy and interstitialcy mechanisms

4.1 Introduction

Nuclear spin relaxation rates due to translational diffusion in solids depend on the details of the diffusion, especially the mechanism of diffusion. The relaxation rates due to diffusion by the vacancy mechanism in the cubic lattices have been well studied using Monte Carlo simulations of the vacancy motion (Wolf 1974; Wolf *et al.* 1977), and approximations to the atomic displacement probabilities based on random walk theory (Sholl 1974, 1982; MacGillivray and Sholl 1986). Additionally, accurate analytic expressions for the atomic displacement probabilities due to the vacancy diffusion mechanism—which are exact in the low vacancy-concentration limit—have been derived by Sholl (1992). Relaxation rates due to the interstitialcy mechanism have not received as much attention, although relaxation rates for diffusion by the forward noncollinear interstitialcy mechanism in a fluorite lattice have been calculated using Monte Carlo simulations of the interstitial defect motion (Wolf *et al.* 1977; Figueroa *et al.* 1979). These last works investigated the effectiveness of using nuclear spin relaxation rate measurements to distinguish between the different diffusion mechanisms in fluorite lattices, BaF_2 in particular. It was found that nuclear spin relaxation

measurements alone were insufficient to determine the diffusion mechanism.

The aim of the present chapter is to apply the exact calculations of atomic displacement probabilities for diffusion by the vacancy and interstitialcy mechanisms to the calculation of relaxation rates in a lattice with a NaCl structure. The diffusion occurs by the encounter model (Eisenstadt and Redfield 1963) where the diffusion is a random walk of atom-defect encounters, the details of each encounter depending on the particular diffusion mechanism being considered. The theory is exact in the low defect-concentration limit.

The particular system to be studied is the relaxation of F nuclei in the ionic solid LiF due to the diffusion of the Li nuclei. The F nuclei are assumed to remain fixed at their f.c.c. lattice sites while the Li nuclei are free to diffuse by either the interstitialcy mechanism or the vacancy mechanism. The Li nuclei diffuse on a f.c.c. lattice by the vacancy mechanism and on a f.c.c.(t) system (see previous chapter) by the interstitialcy mechanism, where each interstitial site is at the centre of the tetrahedron formed by adjacent f.c.c. lattice sites. The mobility of the F nuclei is significantly less than that of the much lighter Li nuclei (Philibert 1991) so when considering the Li–F interactions a reasonable approximation is that the F nuclei are immobile and that only the Li nuclei diffuse. The F nuclei have spin 1/2 and so have zero electric quadrupole moment while both the F and Li nuclei have magnetic dipole moments. The dominant Li–F interaction is therefore magnetic dipolar, and there is no electric quadrupole interaction. The F–F interactions are also magnetic dipolar and will contribute to the relaxation of the fluorine nuclei. It is likely that relaxation due to this interaction will be negligible because of the low mobility of the fluorine nuclei, and in spite of the approximately 25% larger coefficient in the expressions (2.8) for the like-spin (F–F) interaction relaxation rates than in the expressions (4.5) below for the unlike-spin (Li–F) interaction relaxation rates in the present system.

Also developed in this chapter are simple analytic expressions for the spectral density functions of unlike-spin, magnetic dipole interactions when one spin-species is fixed and the other is diffusing by either the interstitialcy or vacancy mechanism in any crystal with the NaCl structure. These expressions facilitate the rapid calculation of relaxation rates due to unlike-spin, magnetic dipole interactions in any solid with the NaCl structure.

4.2 Relaxation rate theory

The nuclear spin relaxation rates can be written as linear combinations of spectral density functions $J^{(p)}(\omega)$. The expressions for the longitudinal relaxation rates in the laboratory frame and in the rotating frame of reference, R_1 and $R_{1\rho}$ respectively, and the transverse relaxation rate R_2 of nuclei with spin number I, due to magnetic dipole interactions with nuclei with spin number S are (Abragam 1961; Hoodless *et al.* 1971)

$$\begin{aligned}
R_1 &= A_s\left\{\frac{1}{12}J^{(0)}(\omega_I-\omega_S)+\frac{3}{2}J^{(1)}(\omega_I)+\frac{3}{4}J^{(2)}(\omega_I+\omega_S)\right\},\\
R_{1\rho} &= A_s\left\{\frac{1}{6}J^{(0)}(\omega_1)+\frac{1}{24}J^{(0)}(\omega_I-\omega_S)+\frac{3}{4}J^{(1)}(\omega_I)+\frac{3}{2}J^{(1)}(\omega_S)+\frac{3}{8}J^{(2)}(\omega_I+\omega_S)\right\},\\
R_2 &= A_s\left\{\frac{1}{6}J^{(0)}(0)+\frac{1}{24}J^{(0)}(\omega_I-\omega_S)+\frac{3}{4}J^{(1)}(\omega_I)+\frac{3}{2}J^{(1)}(\omega_S)+\frac{3}{8}J^{(2)}(\omega_I+\omega_S)\right\}.
\end{aligned} \tag{4.1}$$

Here the constant parameter $A_s=\gamma_I^2\gamma_S^2\hbar^2S(S+1)\left(\frac{\mu_0}{4\pi}\right)^2$, γ_I and γ_S are the gyromagnetic ratios of the I and S spins respectively, ω_I and ω_S are the corresponding Larmor frequencies in the static applied magnetic field, $\mathbf{B}_0$, and ω_1 is the Larmor frequency of spin I in the applied oscillating magnetic field, $\mathbf{B}_1$.

The $J^{(p)}(\omega)$ are the spectral density functions (Abragam 1961; Sholl 1981b)

$$J^{(p)}(\omega)=cd_p^2\sum_{\alpha,\beta}\frac{Y_{2p}^*(\Omega'_\alpha)}{r_\alpha^3}\frac{Y_{2p}(\Omega'_\beta)}{r_\beta^3}P(\mathbf{r}_\alpha,\mathbf{r}_\beta,\omega) \tag{4.2}$$

where $d_0^2=16\pi/5$, $d_1^2=8\pi/15$, $d_2^2=32\pi/15$, $Y_{2p}(\Omega')$ are spherical harmonics normalised to unity, $\mathbf{r}_\alpha=(r_\alpha,\Omega'_\alpha)$ are vectors separating the interacting spins and c is the probability of finding a spin at $\mathbf{r}_\alpha$ relative to one at the origin. The function $P(\mathbf{r}_\alpha,\mathbf{r}_\beta,\omega)$ is the Fourier transform

$$P(\mathbf{r}_\alpha,\mathbf{r}_\beta,\omega)=2\int_0^\infty P(\mathbf{r}_\alpha,\mathbf{r}_\beta,t)\cos\omega t\,dt \tag{4.3}$$

of $P(\mathbf{r}_\alpha,\mathbf{r}_\beta,t)$ which is the probability of a pair of spins being separated by $\mathbf{r}_\beta$ a time t after they were separated by $\mathbf{r}_\alpha$. The directions Ω'_α of the spherical harmonics are relative to the direction of the applied magnetic field.

A more convenient form for these expressions is to express them in terms of dimensionless spectral density functions, $g^{(p)}(\omega\tau_e)$, defined in terms of the $J^{(p)}(\omega)$ by

$$g^{(p)}(\omega\tau_e)=\frac{a^6}{c\tau_e}J^{(p)}(\omega), \tag{4.4}$$

where a is the lattice parameter and τ_e is the mean time between atom-defect encounters. Using this definition, and the relation $\omega_I\gamma_S = \omega_S\gamma_I$, the relaxation rates of equations (4.1) can be written

$$R_1 = \frac{A_s c}{a^6\omega_I}\omega_I\tau_e\left\{\frac{1}{12}g^{(0)}([1-\gamma_S/\gamma_I]\omega_I\tau_e) + \frac{3}{2}g^{(1)}(\omega_I\tau_e) + \frac{3}{4}g^{(2)}([1+\gamma_S/\gamma_I]\omega_I\tau_e)\right\},$$

$$R_{1\rho} = \frac{A_s c}{a^6\omega_I}\omega_I\tau_e\left\{\frac{1}{6}g^{(0)}([\mathrm{B_1/B_0}]\omega_I\tau_e) + \frac{1}{24}g^{(0)}([1-\gamma_S/\gamma_I]\omega_I\tau_e) + \frac{3}{4}g^{(1)}(\omega_I\tau_e)\right. \quad (4.5)$$
$$\left. + \frac{3}{2}g^{(1)}([\gamma_S/\gamma_I]\omega_I\tau_e) + \frac{3}{8}g^{(2)}([1+\gamma_S/\gamma_I]\omega_I\tau_e)\right\},$$

$$R_2 = \frac{A_s c}{a^6\omega_I}\omega_I\tau_e\left\{\frac{1}{6}g^{(0)}(0) + \frac{1}{24}g^{(0)}([1-\gamma_S/\gamma_I]\omega_I\tau_e) + \frac{3}{4}g^{(1)}(\omega_I\tau_e)\right.$$
$$\left. + \frac{3}{2}g^{(1)}([\gamma_S/\gamma_I]\omega_I\tau_e) + \frac{3}{8}g^{(2)}([1+\gamma_S/\gamma_I]\omega_I\tau_e)\right\}.$$

In this form the relaxation rates are functions of $\omega_I\tau_e$ for each of the two cases of constant ω_I and varying τ_e, and of constant τ_e and varying ω_I while keeping the ratio B_1/B_0 constant. The first case corresponds to experiments where the temperature is varied while the applied magnetic field $\mathbf{B_0}$ is held constant. In the second case the applied magnetic field is varied while the temperature is held constant. Useful comparisons between the relaxation rates for different diffusion mechanisms in the same system can be made by plotting the relaxation rates, in units of either $A_s c/(a^6\omega_I)$ or $A_s c\tau_e/a^6$, as functions of $\omega_I\tau_e$. The choice of units depends on whether ω_I ($\mathbf{B_0}$) or τ_e (temperature) is constant.

The mean time between encounters, τ_e, can be written in terms of the mean time between jumps of the point defect, τ_d (Sholl 1981b). If the concentration of nuclei, c, satisfies the conditions $c \sim 1$ and $c \gg \bar{c}$, where $\bar{c}$ is the concentration of defects, then the expression for the mean time between encounters is

$$\tau_e = \frac{P}{\bar{c}}\,\tau_d, \quad (4.6)$$

where P is the mean number of atom-defect interactions per encounter. In the cases when only Schottky or Frenkel defects are present, the concentration of defects $\bar{c} = 1 - c$ and so the conditions $1 \sim c \gg \bar{c}$ hold for low concentrations of defects in these cases. The value of P can be calculated from simple random walk theory in the case of

vacancy defects or from the atom jump probabilities in the case of interstitial defects and is the mean number of times the defect, undergoing a random walk, visits the origin. For example, $P = 1.3446611$ for a vacancy defect diffusing on a f.c.c. lattice.

The mean time between jumps of a defect, τ_d, often follows an Arrhenius behaviour

$$\tau_d = \tau_0 \exp\left(\frac{E_a}{kT}\right) \tag{4.7}$$

where E_a is an activation energy, k is the Boltzmann constant, T is the temperature, and τ_0 is a constant with the same units as τ_d. In the absence of impurity atoms in the solid, the concentration of defects, $\bar{c}$, also follows an Arrhenius form

$$\bar{c} = \bar{c}_0 \exp\left(\frac{-E_c}{kT}\right) \tag{4.8}$$

where E_c is an activation energy and $\bar{c}_0$ is a constant. Combining the above three equations, multiplying by the Larmor frequency, ω, and taking logarithms gives

$$\log(\omega\tau_e) = \log\left(\frac{\omega P \tau_0}{\bar{c}_0}\right) + \left(\frac{E_a + E_c}{k}\right)\frac{1}{T}. \tag{4.9}$$

A plot of the relaxation rates against $\log(\omega\tau_e)$ is therefore equivalent to a plot against $1/T$ and a comparison of theory with experiment can give the sum of the activation energies, $E_a + E_c$, and the ratio $\tau_0/\bar{c}_0$. This is different to the case of relaxation rates due to the electric quadrupole interaction (Cohen and Reif 1957; Sholl 1993) where the relaxation is directly caused by the diffusion of the point defect and so the probability c is equal to the concentration of defects, $\bar{c}$, and is no longer independent of the temperature. In addition, the encounter model is no longer valid and τ_e is replaced by the defect's mean jump-time, τ_d. The relaxation rates (equations (4.5)), for the quadrupole interaction in cubic structures, plotted as functions of $\log(\omega_I\tau_d)$ are then not equivalent to plots against $1/T$ because of the dependence of the relaxation rates on $c = \bar{c}$.

The dependence of $g^{(p)}(\omega\tau)$ on the orientation of the crystal with respect to the magnetic field direction can be expressed in terms of trigonometric functions of the polar angle (θ, ϕ) of the field direction relative to crystal axes and functions $g_{pp'}(\omega\tau)$ defined, for p and $p' = -2$ to 2, by (Sholl 1986)

$$g_{pp'}(\omega\tau) = \frac{a^6}{\tau}\sum_{\alpha,\beta}\frac{Y^*_{2p}(\Omega_\alpha)}{r^3_\alpha}\frac{Y_{2p'}(\Omega_\beta)}{r^3_\beta}P(\mathbf{r}_\alpha, \mathbf{r}_\beta, \omega), \tag{4.10}$$

where the directions of the spherical harmonics are now relative to axes fixed in the crystal. In the present case the axes are chosen to be the xyz-axes in the directions of lines joining adjacent Li and F atoms in the LiF crystal.

The maximum number of independent nonzero parameters needed to specify $g^{(p)}(\omega\tau)$ for each $\omega\tau$ is 15 and crystal symmetry reduces this number (Sholl 1986). In the present case of cubic symmetry the number of independent parameters is two and the angular dependence of the $g^{(p)}(\omega\tau)$ in terms of θ and ϕ is

$$d_p^{-2} g^{(p)}(\omega\tau) = C_1^{(p)} + C_2^{(p)}(\sin^2 2\theta + \sin^4\theta \sin^2 2\phi), \tag{4.11}$$

where

$$C_1^{(0)} = g_{00} \qquad C_1^{(1)} = g_{11} \qquad C_1^{(2)} = \tfrac{1}{2}(g_{00} + g_{11})$$
$$C_2^{(0)} = \tfrac{3}{4}(g_{11} - g_{00}) \quad C_2^{(1)} = -\tfrac{2}{3}C_2^{(0)} \qquad C_2^{(2)} = \tfrac{1}{6}C_2^{(0)}.$$

Since the relaxation rates are linear combinations of the $g^{(p)}(\omega\tau)$ the relaxation rates have the same functional form as the $g^{(p)}(\omega\tau)$ for their orientational dependence on the magnetic field direction.

The spherical average of the spectral density functions over all magnetic field directions, $\langle g_{pp'}(\omega\tau)\rangle$, is

$$\langle g_{pp'}(\omega\tau)\rangle = \frac{d_p^2}{5}\left[2g_{00}(\omega\tau) + 3g_{11}(\omega\tau)\right] \tag{4.12}$$

in all cases. The relaxation rates of polycrystalline solids are often approximated by the spherical average over all magnetic field directions of the appropriate relaxation rates of a single crystal (Barton and Sholl 1976). The spherical averages of the relaxation rates can be written as linear combinations of spherical averages of the spectral density functions similar to those for single crystals (equations (4.5)).

4.3 Diffusion models

The encounter model of diffusion has been widely used to calculate the nuclear magnetic spectral density functions. In this model, diffusion of an atom occurs by a series of atom-defect encounters, each encounter causing a displacement $\boldsymbol{l}$ of the atom with probability $W(\boldsymbol{l})$. In three dimensions an atom-defect encounter consists of a finite number of atom-defect interactions, where the defect causes a displacement of the

atom before it diffuses from the atom, never to return, and the next encounter commences with the first interaction of the atom with another defect. The time between encounters, τ_e, is assumed to be much greater than the duration of an encounter and this theory is therefore exact only in the low defect-concentration limit where the probability that a second atom-defect encounter commences before the completion of the first atom-defect encounter is negligible. The diffusion of the atom proceeds by a simple random walk of such encounters and this model is used to evaluate the probability function $P(\mathbf{r}_\alpha, \mathbf{r}_\beta, t)$, used in calculating the spectral density functions.

In the present case, where one nuclear spin species is fixed while the other is free to diffuse, the probability, $P(\mathbf{r}_\alpha, \mathbf{r}_\beta, t)$, that the two unlike nuclear spins are separated by $\mathbf{r}_\beta$ at time t if they were initially separated by $\mathbf{r}_\alpha$ is equal to the probability, $P(\mathbf{r}_\alpha - \mathbf{r}_\beta, t)$, that the diffusing nucleus is displaced by $\mathbf{r}_\alpha - \mathbf{r}_\beta$ in time t. The probability $P(\mathbf{r}_\alpha, \mathbf{r}_\beta, t)$ will depend on the mean time between encounters, τ_e, and on the mechanism of diffusion, through the atomic displacement probability, $W(\boldsymbol{l})$.

In the following, the evaluation of the spectral density functions is discussed for the encounter model for diffusion by the interstitialcy and vacancy mechanisms, and also for the commonly-used BPP approximation.

4.3.1 BPP model

The BPP model for the spectral density functions is based on an approximation for $P(\mathbf{r}_\alpha, \mathbf{r}_\beta, t)$ which corresponds to the pair of spins maintaining their relative separation for a mean time τ and assuming that the correlation in their dipolar interaction is completely destroyed when a jump of one of the spins occurs. It is therefore equivalent to choosing $P(\mathbf{r}_\alpha, \mathbf{r}_\beta, t)$ to be $\delta_{\alpha\beta}\exp(-t/\tau)$. In keeping with the encounter model for diffusion the parameter τ is τ_e, the mean time between encounters. The resulting dimensionless spectral density functions, $g_{pp'}(\omega\tau)$, for the BPP model are

$$g_{pp'}(\omega\tau) = \frac{2}{1+(\omega\tau)^2} S_{pp'}, \tag{4.13}$$

where $S_{pp'}$ is the dimensionless lattice summation

$$S_{pp'} = a^6 \sum_\alpha \frac{Y^*_{2p}(\Omega_\alpha) Y_{2p'}(\Omega_\alpha)}{r^6_\alpha}. \tag{4.14}$$

The values of S_{00} and S_{11} for the Li–F interaction in LiF are 9.77204 and 0.483012 respectively. This BPP model is widely used in analysing nuclear spin relaxation data, despite the approximations inherent in it, due to the simplicity of using the resulting spectral density functions.

4.3.2 Interstitialcy and vacancy mechanisms

The lattice sums in equation (4.10) for the dimensionless spectral density function $g_{pp'}(\omega\tau)$ converge very slowly for probability functions $P(\mathbf{r}_\alpha, \mathbf{r}_\beta, t)$ corresponding to the encounter model for the interstitialcy and vacancy mechanisms. Spatial Fourier transform techniques speed up the rate of convergence and the spectral density functions can be written

$$g_{pp'}(\omega\tau) = \frac{a^6}{\tau}\frac{v^2}{(2\pi)^6}\iint T_p^*(\boldsymbol{q})T_{p'}(\boldsymbol{q}')P(\boldsymbol{q},\boldsymbol{q}',\omega)\,d\boldsymbol{q}\,d\boldsymbol{q}', \tag{4.15}$$

where the integrals are over the first Brillouin zone (see Appendix A), v is the volume of the unit cell of the real lattice, and $P(\boldsymbol{q},\boldsymbol{q}',\omega)$ is the spatial and temporal Fourier transform of the probability function $P(\mathbf{r}_\alpha, \mathbf{r}_\beta, t)$. The function $T_p(\boldsymbol{q})$ is defined by

$$T_p(\boldsymbol{q}) = \sum_{\boldsymbol{m}} \frac{Y_{2p}(\Omega_\alpha)}{r_\alpha^3}\exp(i\boldsymbol{q}\cdot\mathbf{r}_\alpha), \tag{4.16}$$

where the separation between two interacting spins, $\mathbf{r}_\alpha = \boldsymbol{m} + \boldsymbol{j}$; $\boldsymbol{m}$ is a f.c.c. lattice vector and $\boldsymbol{j}$ is the relative displacement between the two f.c.c. sublattices in the NaCl structure. In its present form the lattice sum in the above expressions for $T_p(\boldsymbol{q})$ converges too slowly to evaluate by a direct summation. Instead the technique used is a planewise summation method which makes use of the Poisson summation formula (Barton and Sholl 1980) and the resulting expressions for $T_p(\boldsymbol{q})$ are given in Appendix B.2.

The general form for $P(\boldsymbol{q},\boldsymbol{q}',\omega)$, when diffusion is by a random walk with a mean time τ between steps, is

$$P(\boldsymbol{q},\boldsymbol{q}',\omega) = \frac{2\tau(2\pi)^3[1-W(\boldsymbol{q})]}{[1-W(\boldsymbol{q})]^2+(\omega\tau)^2}\delta(\boldsymbol{q}-\boldsymbol{q}'), \tag{4.17}$$

where $W(\boldsymbol{q})$ is the spatial Fourier transform,

$$W(\boldsymbol{q}) = \sum_{\boldsymbol{l}} W(\boldsymbol{l})\exp(i\boldsymbol{q}\cdot\boldsymbol{l}), \tag{4.18}$$

of $W(\boldsymbol{l})$, the probability that a step of the random walk has displacement $\boldsymbol{l}$. In the encounter model the diffusion proceeds by an uncorrelated random walk of atom-defect encounters, each resulting in an atomic displacement $\boldsymbol{l}$ with probability $W(\boldsymbol{l})$, and $\tau = \tau_e$ is the mean time between encounters. For the case of the BPP approximation, $W(\boldsymbol{l}) = \delta_{\boldsymbol{l},0}$ and expression (4.17) becomes

$$P(\boldsymbol{q},\boldsymbol{q}',\omega) = \frac{2\tau_e(2\pi)^3}{1+(\omega\tau_e)^2}\delta(\boldsymbol{q}-\boldsymbol{q}'). \tag{4.19}$$

Substituting this expression into equation (4.15) for the spectral density function, $g_{pp'}(\omega\tau)$, gives expression (4.13) of the BPP model.

The expression for $W(\boldsymbol{q})$ for diffusion by the interstitialcy mechanism was derived in the preceding chapter (equation (3.41)) and is

$$W(\boldsymbol{q}) = \frac{(1-p)}{Z}\sum_{i,j,k=1}^{Z_T} Q^{\mathrm{I}}_{jk}\left[\mathbf{I}-p\mathbf{A}(\boldsymbol{q})\right]^{-1}_{ij}\exp[i\boldsymbol{q}\cdot(\boldsymbol{c}_j+\boldsymbol{c}_k)] \tag{4.20}$$

where $Z_T = Z = 8$ is the number of nearest interstitial sites to a normal lattice site, the $\boldsymbol{c}_j$ are the vectors from a normal lattice site to its neighbouring interstitial sites, p is the probability that the defect returns to the atom, and $\mathbf{I}$ is the $Z_T \times Z_T$ identity matrix. The square matrix $\mathbf{A}(\boldsymbol{q})$ has elements

$$A_{ij}(\boldsymbol{q}) = \frac{1}{p}\sum_{k=1}^{Z_T} Q^{\mathrm{I}}_{ik}Q^{\mathrm{N}}_{kj}\exp\left[i\boldsymbol{q}\cdot(\boldsymbol{c}_i+\boldsymbol{c}_k)\right], \tag{4.21}$$

where the $Q^{\mathrm{I}}_{ik} = 1/Z'$ if a jump in the direction $\boldsymbol{c}_i$ from an interstitial (I) to a normal (N) site is possible, or 0 if it is not possible, given that the preceding N to I jump was in the direction $\boldsymbol{c}_k$; and Q^{N}_{kj} is the probability that an N to I jump of an atom is in the direction $\boldsymbol{c}_k$ if the immediately preceding I to N jump was in the direction $\boldsymbol{c}_j$. In the present case of LiF (a f.c.c.(t) system) the number of nearest normal sites to an interstitial site, $Z' = 4$, and $Q^{\mathrm{I}}_{ik} = \frac{1}{4}\delta_{1,(-)^{i+k+1}}$ if the $\boldsymbol{c}_i$ are defined as on page 55. The technique for calculating Q^{N}_{kj} for various interstitialcy mechanisms is discussed in §3.2.2 of the previous chapter.

The corresponding expression for $W(\boldsymbol{q})$ for the vacancy mechanism of diffusion is (Sholl 1992)

$$W(\boldsymbol{q}) = \frac{(1-p)}{Z_a}\sum_{i,j=1}^{Z_a}\left[\mathbf{I}-p\mathbf{A}(\boldsymbol{q})\right]^{-1}_{ij}\exp\left(i\boldsymbol{q}\cdot\boldsymbol{a}_j\right), \tag{4.22}$$

where $Z_a = 12$ is the coordination number of a f.c.c. lattice, $\boldsymbol{a}_j$ is the vector to the j^{th} nearest neighbour lattice site, $\mathbf{I}$ is the $Z_a \times Z_a$ identity matrix and $\mathbf{A}(\boldsymbol{q})$ is the square matrix with elements

$$A_{ij}(\boldsymbol{q}) = \frac{Q_{ij}}{p} \exp(i\boldsymbol{q} \cdot \boldsymbol{a}_i) \tag{4.23}$$

where Q_{ij} is the probability that the next step of the atom will be in the direction $\boldsymbol{a}_i$ if the previous step was in the direction $\boldsymbol{a}_j$. The evaluation of the Q_{ij} was discussed by Sholl.

These expressions for $W(\boldsymbol{q})$ can be used with equations (4.15) and (4.17) to calculate the spectral density functions for the vacancy and interstitialcy mechanisms of diffusion. The Brillouin zone integral in equation (4.15) is evaluated numerically using the Gauss-Legendre quadrature technique.

4.4 Results

Presented below are numerical results of the calculation of the magnetic dipole spectral density functions and relaxation rates of F nuclei in solid LiF due to the diffusion of Li nuclei. The spectral density function results are equally applicable to unlike-spin, magnetic dipole interactions for analogous cationic diffusion in NaCl structures. The results are for diffusion by the collinear, forward- and backward-noncollinear interstitialcy mechanisms and the vacancy mechanism. Other interstitialcy mechanisms are possible and the above were chosen as representative examples of diffusion by the interstitialcy mechanism.

4.4.1 Spectral density functions

The spectral density functions for diffusion by the vacancy and interstitialcy mechanisms in the NaCl structure can be evaluated from equation (4.15) as discussed in §4.3.2. The integrals over the first Brillouin zone in this equation are evaluated numerically to the desired accuracy, for any value of $\omega\tau$, using the Gauss-Legendre quadrature technique. For low values of $\omega\tau$ ($\lesssim 0.01$), where the computing time required to calculate the $g_{pp'}(\omega\tau)$ becomes prohibitively long and the rounding errors

become significant, the low-frequency analytic form is used to calculate the spectral density functions accurately as follows.

The behaviour of expression (4.15) for $g_{pp'}(\omega\tau)$ when $\omega\tau$ is small is dominated by the behaviour of the integrand for small values of $\boldsymbol{q}$ (Sholl 1981a) since

$$\lim_{\boldsymbol{q}\to 0} W(\boldsymbol{q}) = 1 \tag{4.24}$$

and, from equation (4.17), $P(\boldsymbol{q},\boldsymbol{q}',\omega)/\tau$ becomes very large as $\boldsymbol{q} \to 0$ and when $\omega\tau$ is small.

The behaviour of $W(\boldsymbol{q})$ for small $\boldsymbol{q}$ can be found from expressions (4.20) and (4.22) for the interstitialcy and vacancy mechanisms of diffusion. The small-$\boldsymbol{q}$ behaviour can be found by using a symbolic mathematics computer package, and the Taylor expansions for the inverse matrix and the cosine function. When terms in q of order greater than 2 are neglected, the small-$\boldsymbol{q}$ behaviour of $W(\boldsymbol{q})$ is found to be

$$W(\boldsymbol{q}) \to 1 - Fq^2 \tag{4.25}$$

where $F = f/[Z(1-p)]$ for diffusion by the interstitialcy mechanism, and $F = 2f/[Z_a(1-p)]$ for diffusion by the vacancy mechanism, where f is the tracer correlation factor, $Z = 8$ is the number of nearest neighbour interstitial sites to any normal lattice site, $Z_a = 12$ is the coordination number of the f.c.c. sublattice, and p is the probability of the defect returning to an atom.

Low values of $\omega\tau$ correspond to long-range diffusion of the atom where the spatial microscopic details of the diffusion are not important and so in this limit the lattice summations in equation (4.15) for $g_{pp'}(\omega\tau)$ can be replaced with integrals over real space, corresponding to a continuum of an equivalent density of lattice sites. Following the method of Sholl (1981a) the low-frequency limiting form of the spectral density functions can then be written

$$g_{pp'}(\omega\tau) = g_{pp'}(0) - \delta_{pp'}\frac{2}{9}F^{-3/2}\sqrt{\omega\tau} + o(\sqrt{\omega\tau}), \tag{4.26}$$

where $o(\sqrt{\omega\tau})$ refers to terms which vanish faster than $\sqrt{\omega\tau}$ as $\omega\tau \to 0$. As with diffusion in all the cubic lattices the spectral density functions behave as $b - m\sqrt{\omega\tau}$ in the low-frequency limit, where b and m are constants, and the expressions for F for the interstitialcy and vacancy mechanisms in the NaCl structure are given

Table 4.1: Values of the coefficients in the low-frequency approximation (equation (4.26)) of the spectral density functions $g_{pp'}(\omega\tau)$, $p = p' = 0$ and 1 for various mechanisms of diffusion in the NaCl structure. The interaction is magnetic dipolar between the unlike spins of the two f.c.c. sublattices.

	$g_{00}(0)$	$g_{11}(0)$	$\frac{2}{9}F^{-3/2}$
Vacancy	21.75	2.805	3.032093
Collinear interstitialcy, $w_1 = 1$	26.40	3.527	4.372607
Forward noncollinear interstitialcy, $w_2 = 1$	24.34	2.772	2.614965
Backward noncollinear interstitialcy, $w_3 = 1$	23.24	2.359	1.770048

above. The values of the $g_{pp'}(\omega\tau)$ at $\omega\tau = 0$ cannot be found directly, but can be obtained by fitting the above low-frequency forms to the numerical results over the region of small $\omega\tau$ values when $g_{pp'}(\omega\tau)$ shows the $\sqrt{\omega\tau}$ behaviour. The results for some interstitialcy mechanisms and the vacancy mechanism of diffusion are shown in Table 4.1. The low-frequency approximations can be used to determine the $g_{pp'}(\omega\tau)$ for $\omega\tau \leq 0.01$ to within 1% accuracy.

In the high-frequency limit ($\omega\tau \gg 1$) it is necessary to consider only zero or one possible encounter (Barton and Sholl 1980) in which case the spectral density functions can be written

$$g_{pp'}(\omega\tau) \approx \frac{H}{(\omega\tau)^2}, \tag{4.27}$$

where

$$H = \frac{2v}{(2\pi)^3} \int T_p^*(\boldsymbol{q}) T_{p'}(\boldsymbol{q}) \left[1 - W(\boldsymbol{q})\right] \, d\boldsymbol{q}. \tag{4.28}$$

Values for H can be found from expression (4.28) using the Gauss-Legendre quadrature technique to numerically evaluate the integral over the first Brillouin zone. Values of H for $p, p' = 0$ and 1 and for the vacancy and interstitialcy mechanisms are shown in Table 4.2.

Analytic approximations to the numerical results can be useful (Sholl 1988). The function

$$g_{pp'}(\omega\tau) = \frac{H}{a + b(\omega\tau)^{1/2} + c(\omega\tau)^u + d(\omega\tau)^v + (\omega\tau)^2}, \tag{4.29}$$

which incorporates both the high- and low-frequency limiting forms, has been found to fit the results to good accuracy over the entire range of $\omega\tau$, and the values of the parameters and the accuracy of the approximations are given in Table 4.2. These analytic approximations to the spectral density functions provide a useful means of calculating the relaxation rates which are as simple to use as, but without the deficiences of, the BPP approximation.

Table 4.2: Values of the parameters in expression (4.29) for various mechanisms of diffusion of cations in the NaCl structure. The interaction is magnetic dipolar between unlike spins on the different sublattices. The maximum percentage error of each approximation is shown.

	Vacancy		Collinear interstitialcy	
	g_{00}	g_{11}	g_{00}	g_{11}
H	19.7377	0.60411	16.4279	0.49042
a	0.90731	0.21539	0.62230	0.13903
b	0.12646	0.23285	0.10308	0.17234
c	0.29332	0.90717	0.12082	0.99356
d	−0.25191	−0.80127	−0.08662	−0.92145
u	1.00	1.00	1.05	1.02
v	1.15	1.16	1.34	1.14
% error	0.45	2.27	0.59	2.26
	Forward noncollinear interstitialcy		Backward noncollinear interstitialcy	
	g_{00}	g_{11}	g_{00}	g_{11}
H	17.1197	0.55748	17.5344	0.60425
a	0.70327	0.20110	0.75456	0.25618
b	0.07555	0.18969	0.05748	0.19224
c	0.08041	0.89911	0.05060	1.24505
d	−0.05417	−0.83939	−0.02838	−1.19409
u	0.88	1.005	0.85	1.01
v	1.20	1.129	1.25	1.09
% error	0.35	2.03	0.31	1.83

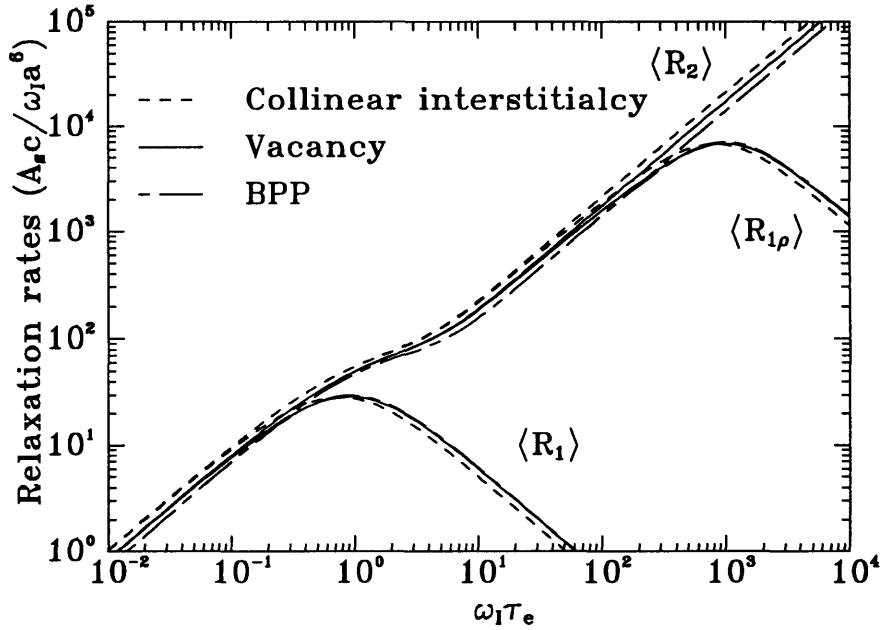

Figure 4.1: The spherical average of all possible magnetic field directions of the relaxation rates R_1, $R_{1\rho}$ and R_2 of F nuclei in solid LiF due to the diffusion of the Li nuclei by the collinear interstitialcy, vacancy and BPP models.

4.4.2 Relaxation rates

The expressions given above for the spectral density functions can be used to calculate the nuclear spin relaxation rates R_1, $R_{1\rho}$ and R_2 which are linear combinations of the spectral density functions, and the details are given in equations (4.5). The relaxation rates are dimensionless when expressed in units of $A_s c/(\omega_I a^6)$ and in all the following the value of the ratio B_0/B_1 is 10^3. Shown in Figures 4.1 to 4.3 are the relaxation rates of the fluorine nuclei, due to the diffusion of the lithium nuclei in LiF, as functions of $\log(\omega_I \tau_e)$ which is equivalent to $1/T$ if the jump rates follow an Arrhenius behaviour with temperature, T. The ratio of gyromagnetic ratios, γ_S/γ_I, which appears in the expressions (4.5) for the relaxation rates is, for the LiF system composed of Li^7 and F^{19} nuclei, $\gamma_{Li}/\gamma_F = 0.41310$. If the analytic approximation (4.29) to the spectral density functions and the values of the parameters given in Table 4.2 are used it is relatively straightforward to reproduce the following results for the relaxation rates.

The spherical average of the relaxation rates due to the collinear interstitialcy mechanism, the vacancy mechanism and also for the BPP approximation are shown in Figure 4.1. In the low-frequency limit the three relaxation rates are linear in

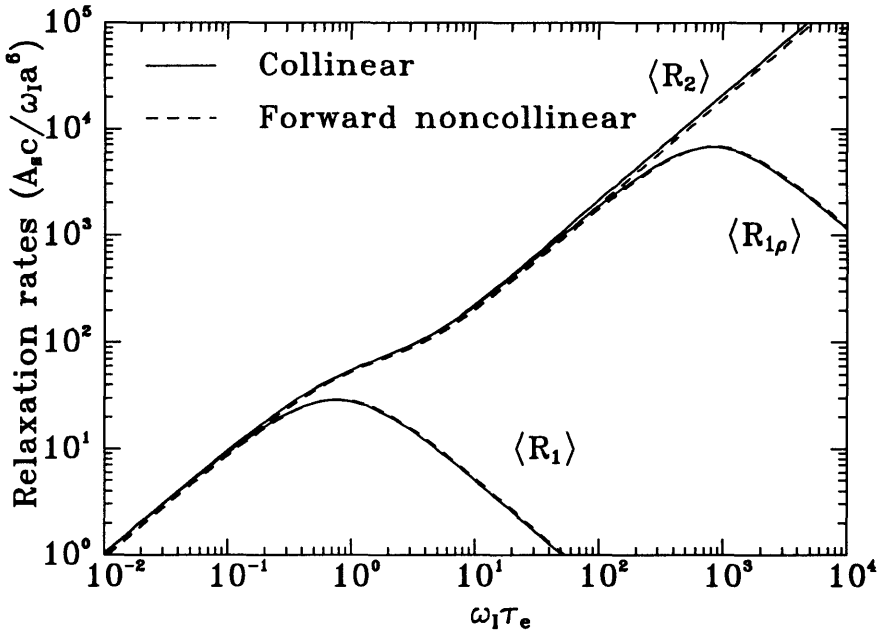

Figure 4.2: The spherical average of all possible magnetic field directions of the relaxation rates R_1, $R_{1\rho}$ and R_2 of F nuclei in solid LiF due to the diffusion of the Li nuclei by the collinear and forward noncollinear interstitialcy mechanisms.

$\omega_I\tau_e$ and $R_1 = R_{1\rho} = R_2$ for each model. At low frequencies ($\omega_I\tau_e \lesssim 0.03$) the difference between the relaxation rates of the collinear interstitialcy and vacancy mechanisms, and between the relaxation rates of the vacancy mechanism and the BPP approximation, is approximately 22%. At high frequencies ($\omega_I\tau_e \gtrsim 7$ for $\langle R_1\rangle$ and $\omega_I\tau_e \gtrsim 3 \times 10^3$ for $\langle R_{1\rho}\rangle$) the $\langle R_1\rangle$ and $\langle R_{1\rho}\rangle$ relaxation rates for the BPP model are indistinguishable in the figure from the corresponding relaxation rates for the vacancy model as there is only 2% difference between the results of the two models. There is a difference of 20% between the collinear interstitialcy and vacancy results for these relaxation rates. The BPP model is therefore a good approximation to the longitudinal relaxation rates (R_1 and $R_{1\rho}$) at high frequencies for diffusion by the vacancy mechanism, but not the interstitialcy mechanism. The high-frequency behaviour of the longitudinal relaxation rates is $1/(\omega_I\tau_e)$ for all the models of diffusion. The differences between the collinear interstitialcy and vacancy, and the vacancy and BPP relaxation rates $\langle R_2\rangle$ are both approximately 22% for $\omega_I\tau_e \gtrsim 10^3$.

Shown in Figure 4.2 are the spherical averages of the relaxation rates due to the collinear ($w_1 = 1$) and forward noncollinear ($w_2 = 1$) interstitialcy mechanisms.

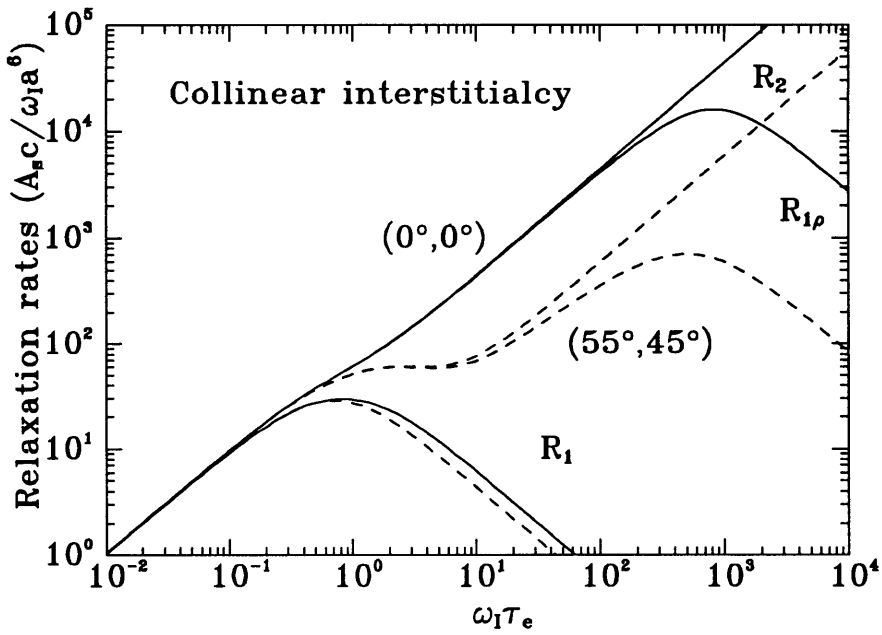

Figure 4.3: The relaxation rates R_1, $R_{1\rho}$ and R_2 of F nuclei in a single crystal of LiF due to the diffusion of the Li nuclei by the collinear interstitialcy mechanism. Relaxation rates corresponding to two different orientations (θ, ϕ) of the applied magnetic field, $\mathbf{B}_0$, are shown.

The differences between the results for the different interstitialcy mechanisms are not as great as those between the collinear interstitialcy and vacancy mechanisms, but are significant nonetheless. At low frequencies ($\omega_I \tau_e \lesssim 0.03$) the differences are approximately 11% as they are also at high frequencies for the relaxation rate $\langle R_2 \rangle$ ($\omega_I \tau_e \gtrsim 10^3$). The corresponding high-frequency differences for $\langle R_1 \rangle$ and $\langle R_{1\rho} \rangle$ are approximately 5%. The relaxation rates $\langle R_1 \rangle$, $\langle R_{1\rho} \rangle$ and $\langle R_2 \rangle$ for the backward noncollinear ($w_3 = 1$) interstitialcy mechanism differ from those of the forward noncollinear mechanism by no more than 7%, and at high frequencies for $\langle R_1 \rangle$ and $\langle R_{1\rho} \rangle$ the difference is less than 0.5%.

Figure 4.3 shows the relaxation rates R_1, $R_{1\rho}$ and R_2 of a single crystal of LiF at two orientations, $(\theta, \phi) = (0, 0)$ and $(55°, 45°)$, of the applied magnetic field relative to the crystallographic axes. These are orientations which show the range of possible values of the relaxation rates. In the low-frequency limit the relaxation rates are independent of the magnetic field orientation, while at high frequencies the results vary significantly with magnetic field direction. The relaxation rates due to the

vacancy mechanism of diffusion vary with angles θ and ϕ in a similar way to the interstitialcy mechanism shown here. As discussed in §4.2 the relaxation rates are linear combinations of spectral density functions and so have the same dependence on the magnetic field direction, (θ, ϕ), namely

$$A + B(\sin^4\theta + \sin^2 2\theta \sin^4\phi), \tag{4.30}$$

where A and B are linear combinations of the $g_{pp'}(\omega\tau)$ at $\theta = 0$, and numerical values can be calculated for any value of $\omega\tau$. The maximum and minimum of the R_1 maximum of the collinear interstitialcy mechanism for any angles θ and ϕ, in units of $A_s c/(\omega_I a^6)$, are 29.48 at $\theta = 0$ and 28.55 at $\theta = 55°$, $\phi = 45°$. The analogous values of the $R_{1\rho}$ maxima are 15898. at $\theta = 0$ and 705.97 at $\theta = 55°$, $\phi = 45°$. The R_1 and $R_{1\rho}$ maxima for the vacancy are approximately 0.5% larger than the corresponding results of the collinear interstitialcy mechanism, for all angles θ and ϕ.

The positions of the maxima of the longitudinal relaxation rate curves R_1 and $R_{1\rho}$ are important parameters since they can directly give a value of τ_e at the temperature for which the maximum relaxation rate occurs. The positions of the R_1 and $R_{1\rho}$ maxima, as functions of magnetic field orientation (θ, ϕ), for diffusion by the collinear interstitialcy and vacancy mechanisms and the BPP approximation are shown in Figures 4.4 and 4.5. The range of angles shown in these figures ($0 \leq \theta \leq 90°$ and $0 \leq \phi \leq 45°$) is sufficient to specify the results for any orientation, by crystal symmetry. It can be seen from Figure 4.4 that the variation with angle of the position of the R_1 maximum is similar, although there are differences in magnitude, for the collinear interstitialcy mechanism, the vacancy mechanism and the BPP approximation. The corresponding results for the $R_{1\rho}$ maxima are shown in Figure 4.5 where the results for the interstitialcy and vacancy mechanisms again show a similar variation with angle, although with a difference in magnitude. The results for the BPP approximation, however, do not vary from $\omega_I\tau_e = 1000$ by more than 0.3% for any angles, θ and ϕ, and is significantly different in magnitude from the interstitialcy results.

To further investigate the low-frequency behaviour of the relaxation rates it is useful to consider the differences $R_2 - R_{1\rho}$ and $R_{1\rho} - R_1$ between the relaxation rates. From equations (4.5) for the relaxation rates expressions for these differences are

$$R_2 - R_{1\rho} = \frac{A_s c}{a^6\omega_I}\omega_I\tau_e\frac{1}{6}\left\{g^{(0)}(0) - g^{(0)}([\mathrm{B}_1/\mathrm{B}_0]\omega_I\tau_e)\right\}, \tag{4.31}$$

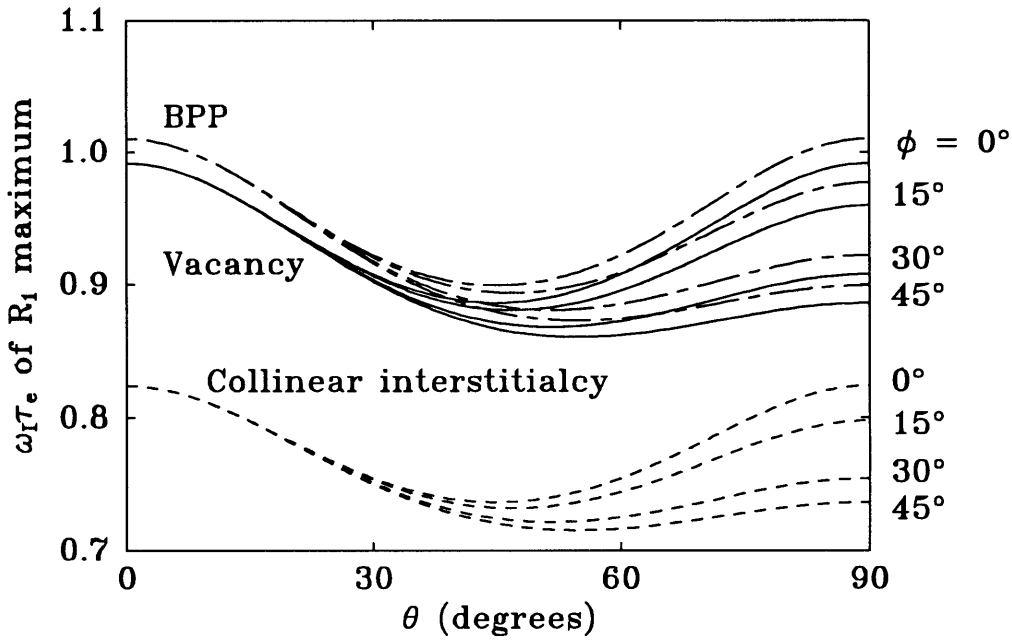

Figure 4.4: The position of the R_1 maxima as functions of the magnetic field orientation (θ, ϕ) for the collinear interstitialcy mechanism, the vacancy mechanism and the BPP approximation.

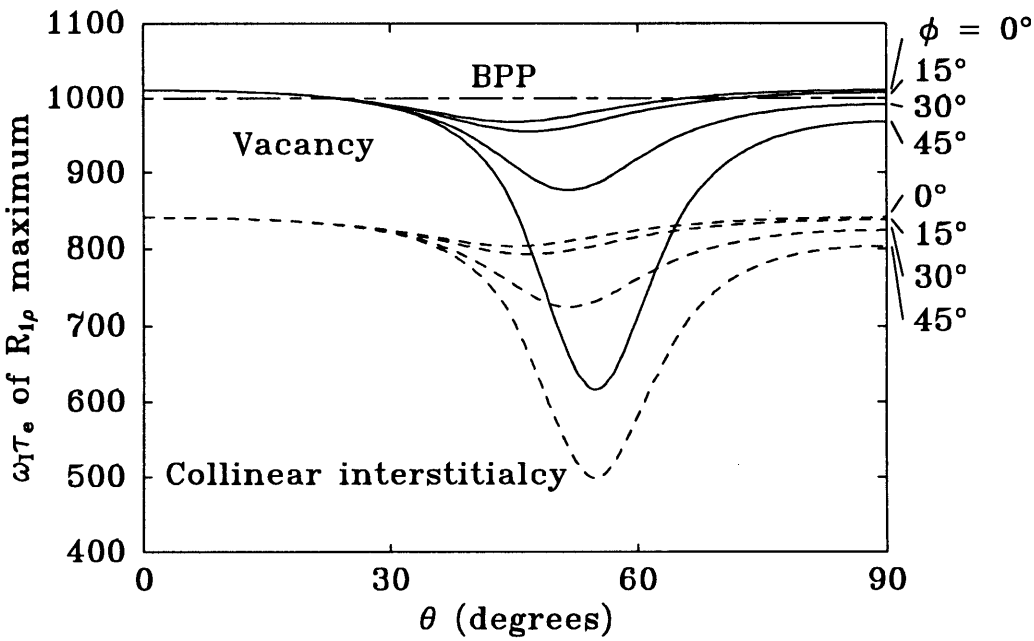

Figure 4.5: The position of the $R_{1\rho}$ maxima as functions of the magnetic field orientation (θ, ϕ) for the collinear interstitialcy mechanism, the vacancy mechanism and the BPP approximation.

$$R_{1\rho} - R_1 = \frac{A_s c}{a^6 \omega_I} \omega_I \tau_e \left\{ \frac{1}{6} g^{(0)}([B_1/B_0]\omega_I\tau_e) - \frac{1}{24} g^{(0)}([1 - \gamma_S/\gamma_I]\omega_I\tau_e) \right. \quad (4.32)$$
$$\left. - \frac{3}{4} g^{(1)}(\omega_I\tau_e) + \frac{3}{2} g^{(1)}([\gamma_S/\gamma_I]\omega_I\tau_e) - \frac{3}{8} g^{(2)}([1 + \gamma_S/\gamma_I]\omega_I\tau_e) \right\},$$

where equation (4.11) can be used to calculate the spectral density functions, $g^{(p)}(\omega\tau)$, in terms of the $g_{pp'}(\omega\tau)$. At low frequencies, where the low-frequency limiting form for the $g_{pp'}(\omega\tau)$ (equation (4.26)) is a good approximation to the vacancy and interstitialcy models, the differences $R_2 - R_{1\rho}$ and $R_{1\rho} - R_1$ are independent of the magnetic field direction and can be written

$$R_2 - R_{1\rho} \approx \frac{A_s c}{\omega_I a^6} \frac{2}{9} F^{-3/2} \sqrt{\frac{B_1}{B_0}} (\omega_I\tau_e)^{3/2}, \quad (4.33)$$

$$R_{1\rho} - R_1 \approx \frac{A_s c}{\omega_I a^6} \frac{2}{9} F^{-3/2} \frac{4\pi}{5} \left[\frac{1}{2} - \frac{2}{3} \sqrt{\frac{B_1}{B_0}} - \sqrt{\frac{\gamma_S}{\gamma_I}} + \frac{1}{6} \sqrt{1 - \frac{\gamma_S}{\gamma_I}} + \sqrt{1 + \frac{\gamma_S}{\gamma_I}} \right] (\omega_I\tau_e)^{3/2} \quad (4.34)$$

which are proportional to $(\omega_I\tau_e)^{3/2}$. In the low-frequency limit the relaxation rates are proportional to $\omega_I\tau_e$ and so the slope of a logarithmic plot of the difference between relaxation rates against $\omega_I\tau_e$ will be 3/2 times the slope of a corresponding plot of the relaxation rates.

In the case of the BPP model, however, the low-frequency behaviour of the spectral density functions is proportional to $1 - (\omega\tau)^2$, for which the differences between the relaxation rates, $R_2 - R_{1\rho}$ and $R_{1\rho} - R_1$, of the BPP approximation are proportional to $(\omega_I\tau_e)^3$ in the low-frequency limit. A logarithmic plot of the difference between the relaxation rates against $\omega_I\tau_e$ of the BPP approximation will therefore have a slope equal to twice the slope of the corresponding plots for the vacancy and interstitialcy mechanisms.

The spherical average of the relaxation rate differences, $\langle R_2 - R_{1\rho} \rangle$ and $\langle R_{1\rho} - R_1 \rangle$, for the case of relaxation of F nuclei in LiF are shown in Figure 4.6 for the collinear interstitialcy and vacancy mechanisms, with their low-frequency approximations, and the BPP model. It can be seen that the slope of the BPP curves, at low frequencies, is twice the slope of the vacancy and interstitialcy curves. The vacancy and collinear interstitialcy results differ by approximately 30% in the low-frequency limit.

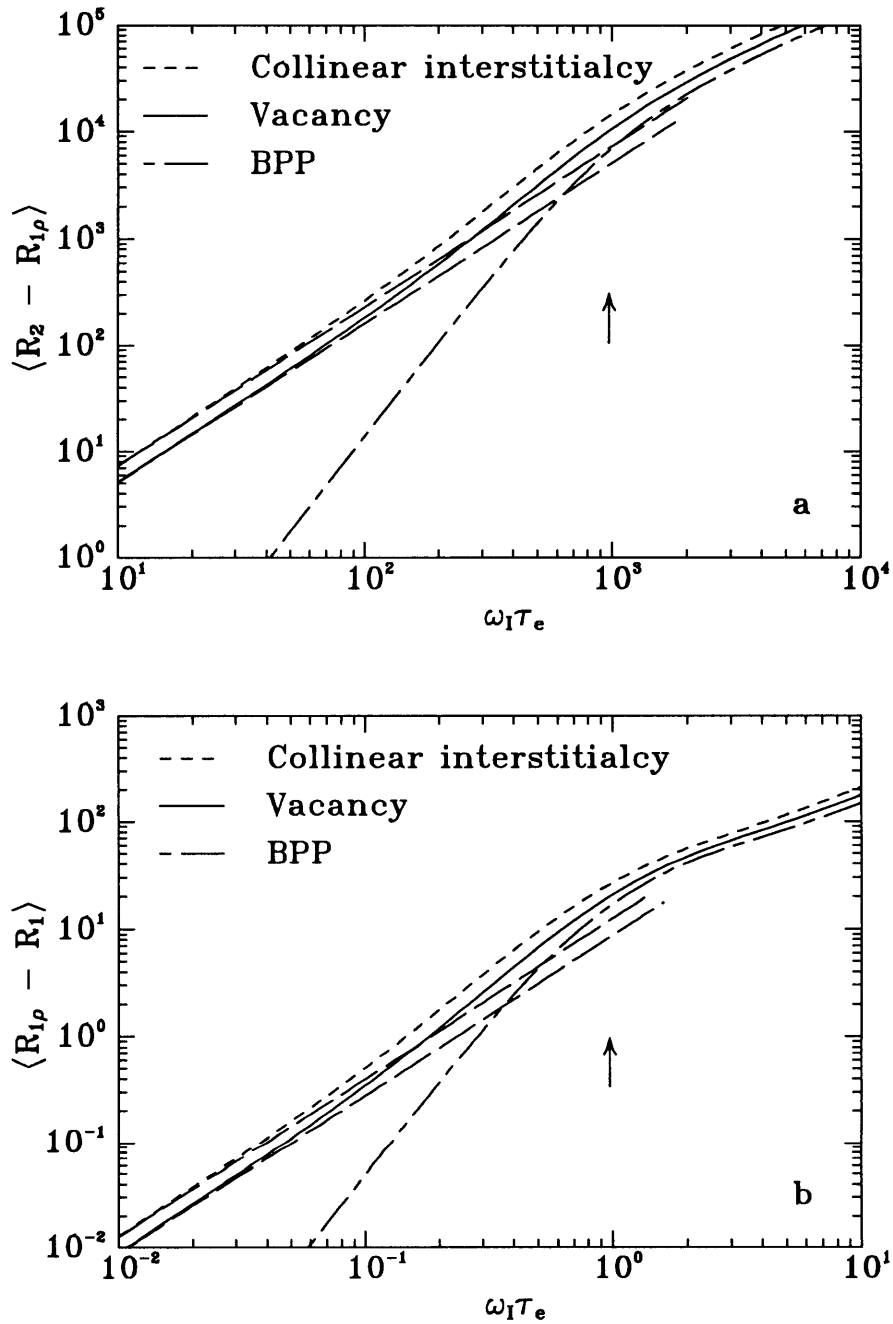

Figure 4.6: The spherical averages of the relaxation rate differences, a) $\langle R_2 - R_{1\rho}\rangle$ and b) $\langle R_{1\rho} - R_1\rangle$, for the collinear interstitialcy mechanism, the vacancy mechanism and the BPP approximation (in units of $A_s c/(\omega_I a^6)$). The long-dashed lines are the low-frequency limiting forms of the interstitialcy and vacancy diffusion, and the arrows indicate the $\omega_I\tau_e$ values of the $R_{1\rho}$ (a) and R_1 (b) maxima.

4.5 Conclusion

Accurate expressions for the atomic displacement probabilities of the interstitialcy mechanism and the vacancy mechanism for diffusion in the NaCl structure have been applied to the theory of nuclear-spin, magnetic dipole relaxation rates due to translational diffusion, exact in the low defect-concentration limit. Analytic approximations to the unlike-spin, magnetic dipole spectral density functions were found and provide an accurate and straightforward means of calculating the relaxation rates in any system with the NaCl structure. The analytic approximation is given by expression (4.29) and the values of the parameters for the vacancy mechanism and some interstitialcy mechanisms are given in Table 4.2.

The relaxation rates of the F nuclei in LiF due to the diffusion of the Li nuclei by the vacancy mechanism and some interstitialcy mechanisms were calculated. The shapes of the equivalent relaxation rate curves for the different mechanisms of diffusion are similar, but there are considerable differences in the horizontal scaling (see Figure 4.1). The behaviour of the relaxation rates, however, as a function of magnetic field orientation is similar for different diffusion mechanisms (see Figures 4.4 and 4.5), and the corresponding values of the R_1 and $R_{1\rho}$ maxima differ by less than 1%. The relaxation rates due to the magnetic dipole interactions, therefore, do not provide an effective way of distinguishing between the vacancy mechanism and the interstitialcy mechanisms of diffusion in LiF; nevertheless, the correct theory for the diffusion mechanism is required to interpret experimental results accurately. This is consistent with the conclusions of Figueroa *et al.* (1979) for the fluorite lattices.

The relaxation rates for the BPP approximation were calculated and found to differ significantly from the corresponding relaxation rates due to the interstitialcy mechanisms, at all frequencies, and the corresponding relaxation rates due to the vacancy mechanism at all but high frequencies (low temperatures). In particular, the variation of the position of the $R_{1\rho}$ maxima with magnetic field orientation is negligible in the case of the BPP approximation, in contrast to the considerable variation of position with orientation in the cases of the vacancy mechanism and interstitialcy mechanisms. The BPP model is therefore a poor approximation to relaxation rates due to diffusion by the vacancy mechanism and interstitialcy mechanisms.

The differences in the low-frequency behaviour between the BPP model and the

vacancy and interstitialcy mechanisms can be clearly seen in logarithmic plots of the relaxation rate differences, $R_2 - R_{1\rho}$ and $R_{1\rho} - R_1$, against $\omega_I \tau_e$. The behaviour for the vacancy and interstitialcy mechanisms is as $(\omega_I \tau_e)^{3/2}$, while the behaviour of the BPP model is $(\omega_I \tau_e)^3$ which is a consequence of the decorrelation after a single jump of the nucleus in this model. It is possible that the $(\omega_I \tau_e)^{3/2}$-behaviour of the vacancy and interstitialcy mechanisms could be experimentally observed at sufficiently low frequencies (high temperatures).

Chapter 5

Conclusion

The preceding chapters describe and discuss work on the study of atomic diffusion in the solid state and its application to nuclear spin relaxation, which is a common experimental technique for the study of diffusion. Atomic diffusion in solids is due, largely, to point defects in the solid which may be of several types and may cause diffusion by several mechanisms. Diffusion studies are therefore important, not only for the information revealed about diffusion parameters, but also for obtaining details about point defects—which in turn affect many of the bulk properties of a solid; such as, electrical and thermal conductivity, mechanical strength, and magnetic properties. In the present work, three aspects of atomic diffusion have been considered: the study of nuclear spin relaxation for the case where the atomic diffusion is restricted to a plane or planes (two-dimensional diffusion), the analysis of diffusion correlation factors and atomic displacement probabilities for the interstitialcy mechanism of three-dimensional diffusion, and a comparison of the form of nuclear spin relaxation rates for some different mechanisms of three-dimensional diffusion.

In Chapter 2, the random walk and mean field theories were applied to the case of diffusion on a square, two-dimensional lattice. The spectral density functions obtained for interactions between atoms confined to planar diffusion is applicable to systems with a layered structure, especially the intercalated compounds, and to systems where surface diffusion is significant. An example where atomic, planar diffusion is significant is in the much studied, superionic conductor Na β-alumina in which the Na^+ ions diffuse in layers of hexagonal networks. In the present work the case of diffusion on a square lattice in the low-concentration limit was considered. The

general results of this system, as discussed in §2.5, can be extended to diffusion in other similar systems—as done in §2.4.2 for diffusion on the hexagonal and honeycomb structures. These generalisations, however, are only approximate and it would be necessary to perform the detailed calculations for diffusion on these structures to determine the exact details of the resulting spectral density functions.

Rigorous calculations of diffusion parameters for diffusion on the hexagonal and honeycomb structures are possible using the methods developed in the present work for the square lattice. The extensions necessary to apply the calculations to diffusion on the hexagonal structure would be straightforward, whereas those for the honeycomb structure are complicated since this structure is not a Bravais lattice. This complication could be overcome with the use of a basis of six atom sites on a hexagonal lattice to describe the honeycomb structure, and a set of appropriate atom jump probabilities to describe the jumps between lattice sites on the different hexagonal lattices.

Chapters 3 and 4 present work on the interstitialcy mechanism of atomic diffusion and on the calculation of the relaxation rates associated with diffusion by the interstitialcy and vacancy mechanisms of self-diffusion of Li in LiF. A method of calculating the atom jump probabilities for each possible jump direction for the general case of diffusion by the interstitialcy mechanism in some two- and three-dimensional structures was given in Chapter 3. The atom jump probabilities are fundamental to the calculation of many diffusion-dependent properties including atomic displacement probabilities and, from these, the observable results of nuclear magnetic relaxation experiments (in addition to neutron scattering, radiotracer and conductivity experiments). The techniques developed here could be applied to other periodic structures, and could be extended to other two-part diffusion mechanisms such as the dumbell interstitialcy mechanism; a common mechanism for diffusion in f.c.c. and b.c.c. metals. Once the atom jump probabilities are known, it is straightforward to calculate the tracer correlation factor for diffusion. This was done, in the present work, for diffusion by the interstitialcy mechanism in various two- and three-dimensional structures in the low defect-concentration limit. The tracer correlation factor makes straightforward comparisons between different mechanisms of diffusion in a structure possible, and was discussed in §3.3 and §3.5.

A specific application of the atomic displacement probabilities, calculated in Chapter 3, to nuclear spin relaxation theory has been presented in Chapter 4. The spectral density functions and nuclear spin relaxation rates of Li nuclei were calculated for the diffusion of Li in LiF, which has the rocksalt structure. The nuclear spin relaxation rates for diffusion by the vacancy mechanism and various types of interstitialcy mechanisms were compared and the results discussed in §4.5. The spectral density functions obtained can also be applied to the calculation of relaxation rates for nuclei in other compounds with the rocksalt structure; such as the silver halides. Cation Frenkel pairs are the predominant defects present in the silver halides. The four possible mechanisms in these systems are the vacancy, direct interstitial, collinear and non-collinear interstitialcy. It is of interest, therefore, to determine which defect has the most significant influence on atomic diffusion within the compound and the dominant mechanism by which the diffusion proceeds. The present work will enable an accurate analysis of results of diffusion experiments in such compounds. The necessity of an accurate and detailed analysis of nuclear spin relaxation theory was demonstrated in the present work, where the differences between the relaxation results of diffusion of Li by the vacancy and interstitialcy mechanisms in LiF were shown to be small. Diffusion in other compounds with the rocksalt structure is likely to be similarly dependent on the diffusion mechanism, in which case a detailed analysis is required to determine the resulting differences due to the diffusion mechanisms and under what conditions these differences could be observed experimentally.